JCI The Journal of Clinical Investigation

Ectodomain shedding of EGFR ligands and TNFR1 dictates hepatocyte apoptosis during fulminant hepatitis in mice

Aditya Murthy, … , Carl P. Blobel, Rama Khokha

J Clin Invest. 2010;120(8):2731-2744. https://doi.org/10.1172/JCI42686.

Research Article **Hepatology**

The cell death receptor Fas plays a role in the establishment of fulminant hepatitis, a major cause of drug-induced liver failure. Fas activation elicits extrinsic apoptotic and hepatoprotective signals; however, the mechanisms by which these signals are integrated during disease are unknown. Tissue inhibitor of metalloproteinases 3 (TIMP3) controls the critical sheddase a disintegrin and metalloproteinase 17 (ADAM17) and may dictate stress signaling. Using mice and cells lacking TIMP3, ADAM17, and ADAM17-regulated cell surface molecules, we have found that ADAM17-mediated ectodomain shedding of TNF receptors and EGF family ligands controls activation of multiple signaling cascades in Fas-induced hepatitis. We demonstrated that TNF signaling promoted hepatotoxicity, while excessive TNF receptor 1 (TNFR1) shedding in *Timp3*$^{-/-}$ mice was protective. Compound *Timp3*$^{-/-}$*Tnf*$^{-/-}$ and *Timp3*$^{-/-}$*Tnfr1*$^{-/-}$ knockout conferred complete resistance to Fas-induced toxicity. Loss of *Timp3* enhanced metalloproteinase-dependent EGFR signaling due to increased release of the EGFR ligands TGF-α, amphiregulin, and HB-EGF, while depletion of shed amphiregulin resensitized *Timp3*$^{-/-}$ hepatocytes to apoptosis. Finally, adenoviral delivery of *Adam17* prevented acetaminophen-induced liver failure in a clinically relevant model of Fas-dependent fulminant hepatitis. These findings demonstrate that TIMP3 and ADAM17 cooperatively dictate cytokine signaling during death receptor activation and indicate that regulated metalloproteinase activity integrates survival and death signals during acute hepatotoxic stress.

Ectodomain shedding of EGFR ligands and TNFR1 dictates hepatocyte apoptosis during fulminant hepatitis in mice

Aditya Murthy,[1] Virginie Defamie,[1] David S. Smookler,[1] Marco A. Di Grappa,[1] Keisuke Horiuchi,[2] Massimo Federici,[3] Maria Sibilia,[4] Carl P. Blobel,[5] and Rama Khokha[1]

[1]Ontario Cancer Institute, Toronto, Ontario, Canada. [2]Department of Orthopedic Surgery and Anti-Aging Orthopedic Research, Keio University, School of Medicine, Tokyo, Japan. [3]Department of Internal Medicine, University of Rome Tor Vergata, Rome, Italy. [4]Medical University of Vienna, Vienna, Austria. [5]Hospital for Special Surgery at Weill Medical College of Cornell University, New York, New York, USA.

The cell death receptor Fas plays a role in the establishment of fulminant hepatitis, a major cause of drug-induced liver failure. Fas activation elicits extrinsic apoptotic and hepatoprotective signals; however, the mechanisms by which these signals are integrated during disease are unknown. Tissue inhibitor of metalloproteinases 3 (TIMP3) controls the critical sheddase a disintegrin and metalloproteinase 17 (ADAM17) and may dictate stress signaling. Using mice and cells lacking TIMP3, ADAM17, and ADAM17-regulated cell surface molecules, we have found that ADAM17-mediated ectodomain shedding of TNF receptors and EGF family ligands controls activation of multiple signaling cascades in Fas-induced hepatitis. We demonstrated that TNF signaling promoted hepatotoxicity, while excessive TNF receptor 1 (TNFR1) shedding in *Timp3*$^{-/-}$ mice was protective. Compound *Timp3*$^{-/-}$*Tnf*$^{-/-}$ and *Timp3*$^{-/-}$*Tnfr1*$^{-/-}$ knockout conferred complete resistance to Fas-induced toxicity. Loss of *Timp3* enhanced metalloproteinase-dependent EGFR signaling due to increased release of the EGFR ligands TGF-α, amphiregulin, and HB-EGF, while depletion of shed amphiregulin resensitized *Timp3*$^{-/-}$ hepatocytes to apoptosis. Finally, adenoviral delivery of *Adam17* prevented acetaminophen-induced liver failure in a clinically relevant model of Fas-dependent fulminant hepatitis. These findings demonstrate that TIMP3 and ADAM17 cooperatively dictate cytokine signaling during death receptor activation and indicate that regulated metalloproteinase activity integrates survival and death signals during acute hepatotoxic stress.

Introduction

Hepatocytes are highly sensitive to death receptor–mediated apoptosis. Engagement of this pathway elicits multiple and complex extrinsic signals, some apoptotic and others hepatoprotective. The cumulative tissue response to these signals determines survival of the organism; however, our understanding of the mechanisms that coordinate them remains incomplete. Mouse models of acute and chronic hepatotoxicity have revealed processes downstream of TNF superfamily receptors such as TNF receptor 1 (TNFR1), Fas/CD95, and death receptors 4 and 5 (DR4, DR5) that direct context-dependant responses. For example, LPS- and concanavalin A–driven hepatitis require TNF signaling. In the LPS model, soluble TNF secreted by components of the immune system, primarily macrophages and neutrophils, drives the destruction of hepatocytes and results in fatal hepatitis, whereas hepatitis caused by concanavalin A is promoted by membrane-bound TNF on T lymphocytes (1). Furthermore, membrane-bound TNF on T cells is protective during *Listeria* and mycobacterial infection (2, 3). Such studies have shown that TNFR1 signals through JNK, NF-κB, and caspases during a stress response, each with significantly different outcome on survival (4–6). In addition to the fundamental role that TNF signaling plays in the above systems, TNF may be a contributing factor in pathologies where it is not the primary stimulus. TNF-related apoptosis-inducing ligand (TRAIL) and its receptor DR4 are known to promote fulminant hepatitis, but there is a lack of conclusive evidence for the function of TNF in Fas-mediated hepatic failure (7).

Even less is known about the role of EGFR signaling during acute hepatic stress. Of the 4 ERBB family members, EGFR/ERBB1 provides critical mitogenic signals through ERK1/2 phosphorylation, and mice lacking EGFR do not survive postnatally (8). Studies have also suggested a protective role for EGFR signaling in models of hepatocyte regeneration and cellular stress induced by ROS or DNA damage (9, 10). However controversy exists regarding the role of EGFR activation in Fas-mediated hepatocyte apoptosis, as some groups have proposed that EGFR interaction with Fas is required for death receptor tyrosine phosphorylation and DISC formation, while others report that EGFR ligands EGF, HB-EGF, and amphiregulin are protective in this model (9, 11–14). Genetic manipulation of EGFR and its modulators is required to establish its function in hepatocyte apoptosis.

TNF, its receptors, and several EGFR ligands are cleaved from the cell surface by a disintegrin and metalloproteinase 17 (ADAM17/TNF-α converting enzyme) in a process termed ectodomain shedding (15, 16). ADAM17-mediated release of EGFR ligands from the cell surface via ectodomain shedding is considered essential for EGFR activation. Binding of soluble ligand exposes a dimerization loop via a conformational change in the EGFR monomer, which is then followed by homodimerization and receptor tyrosine kinase activity. Membrane-bound or uncleavable ligand can therefore impede EGFR activation by preventing dimerization (17, 18). Mice that lack *Adam17* phenocopy *Egfr*$^{-/-}$ mice, pointing to the requirement of this metalloproteinase in EGFR signaling

Conflict of interest: The authors have declared that no conflict of interest exists.
Citation for this article: *J Clin Invest.* 2010;120(8):2731–2744. doi:10.1172/JCI42686.

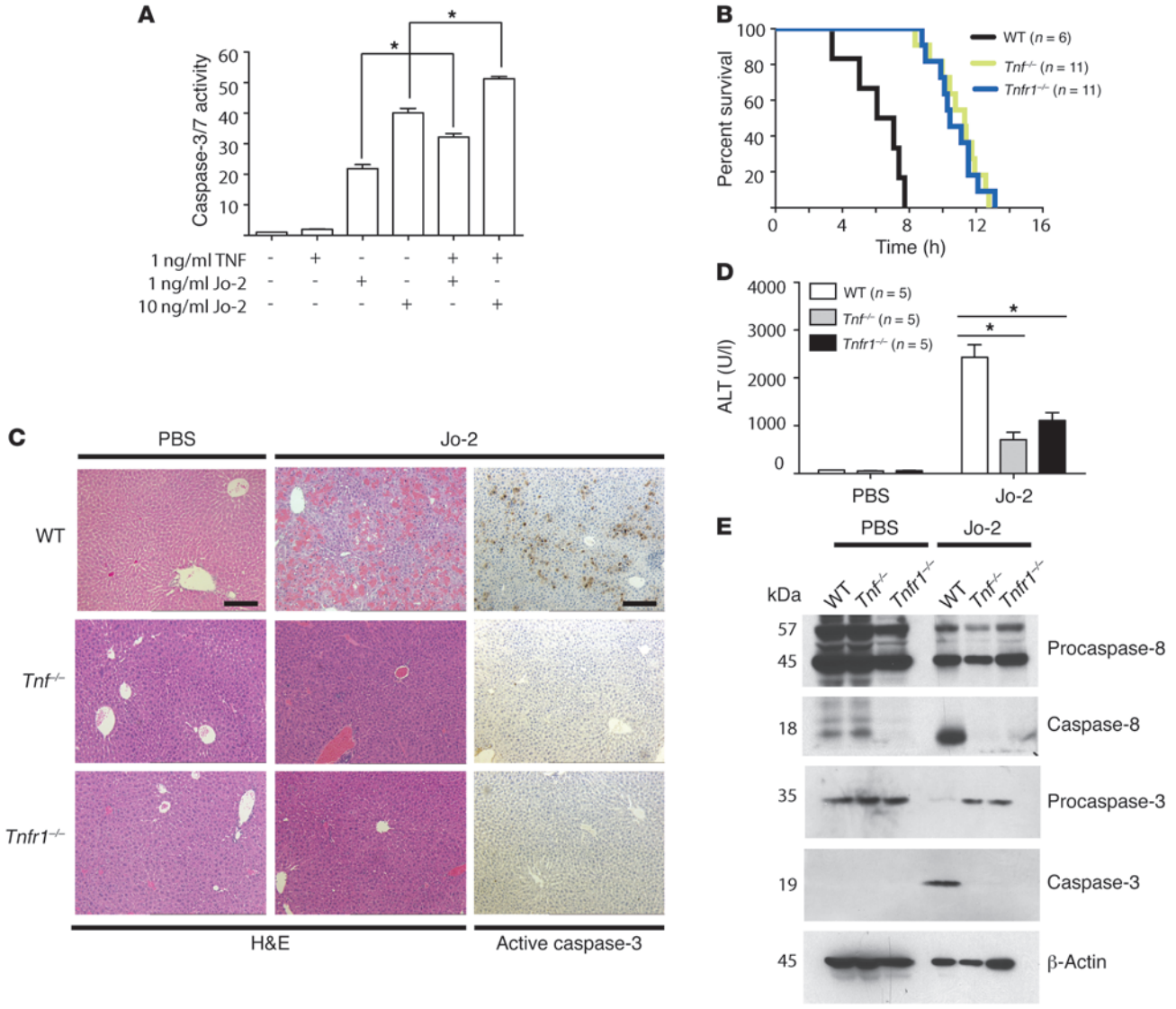

Figure 1

Ablation of TNF signaling delays Fas-mediated hepatotoxicity. (**A**) Apoptosis of wild-type primary hepatocytes treated for 12 hours with the indicated doses of Jo-2 in the presence or absence of 1 ng/ml TNF. Caspase-3/7 activity was measured by rate of cleavage of fluorogenic peptide Ac-DEVD-AMC and represented relative to untreated samples. *$P < 0.03$. Data are mean ± SD ($n = 3$). (**B**) Survival curve of wild-type, *Tnf*$^{-/-}$, and *Tnfr1*$^{-/-}$ mice injected i.p. with 0.65 μg/g Jo-2. $P < 0.005$ versus WT (log-rank test). (**C**–**E**) WT, *Tnf*$^{-/-}$, and *Tnfr1*$^{-/-}$ mice were injected i.p. with 0.65 μg/g Jo-2 or PBS. Mice were sacrificed and tissue obtained 3 hours after injection. (**C**) Liver histology (H&E, active caspase-3 immunohistochemistry) showing absence of tissue damage and caspase-3 activation in *Tnf*$^{-/-}$ and *Tnfr1*$^{-/-}$ mice after treatment with Jo-2. Sections are representative of at least 4 mice per genotype and treatment. Scale bars: 100 μm (**D**) Hepatic toxicity measured by serum ALT levels. *$P \leq 0.04$. Data are mean ± SD ($n = 5$). (**E**) Immunoblots assaying the processing of caspase-8 and -3 in liver lysates. All data are representative of at least 2 independent experiments.

(19). ADAM17 activity is blocked by TIMP3, a stromal inhibitor of several MMPs and ADAMs (20, 21). During inflammation, TIMP3 provides an extracellular mode of controlling TNF-mediated stress response. We have previously reported that TIMP3 checks TNF release and activity during liver regeneration and endotoxin-mediated septic shock (22, 23). Together, the ADAM17/TIMP3 axis may simultaneously affect the opposing signals that determine survival following death receptor activation.

This study investigates stromal control of ectodomain shedding as an integrator of TNF and EGF signaling during Fas-mediated hepatotoxicity. We provide the first in vivo evidence to our knowledge that TNF sensitizes hepatocytes to Fas-mediated death and that increased TNFR1 shedding in TIMP3-deficient mice protects from fulminant hepatitis by dampening TNF activation of JNK, NF-κB, and caspases. We also show that TIMP3 is a negative regulator of EGFR-mediated ERK1/2 phosphorylation, which provides hepatoprotection. Further, this concept applies to a clinically relevant model of drug overdose–induced acute liver failure requiring Fas. TIMP3 regulation of ectodomain shedding is therefore necessary for the apoptotic response during Fas-mediated hepatotoxicity.

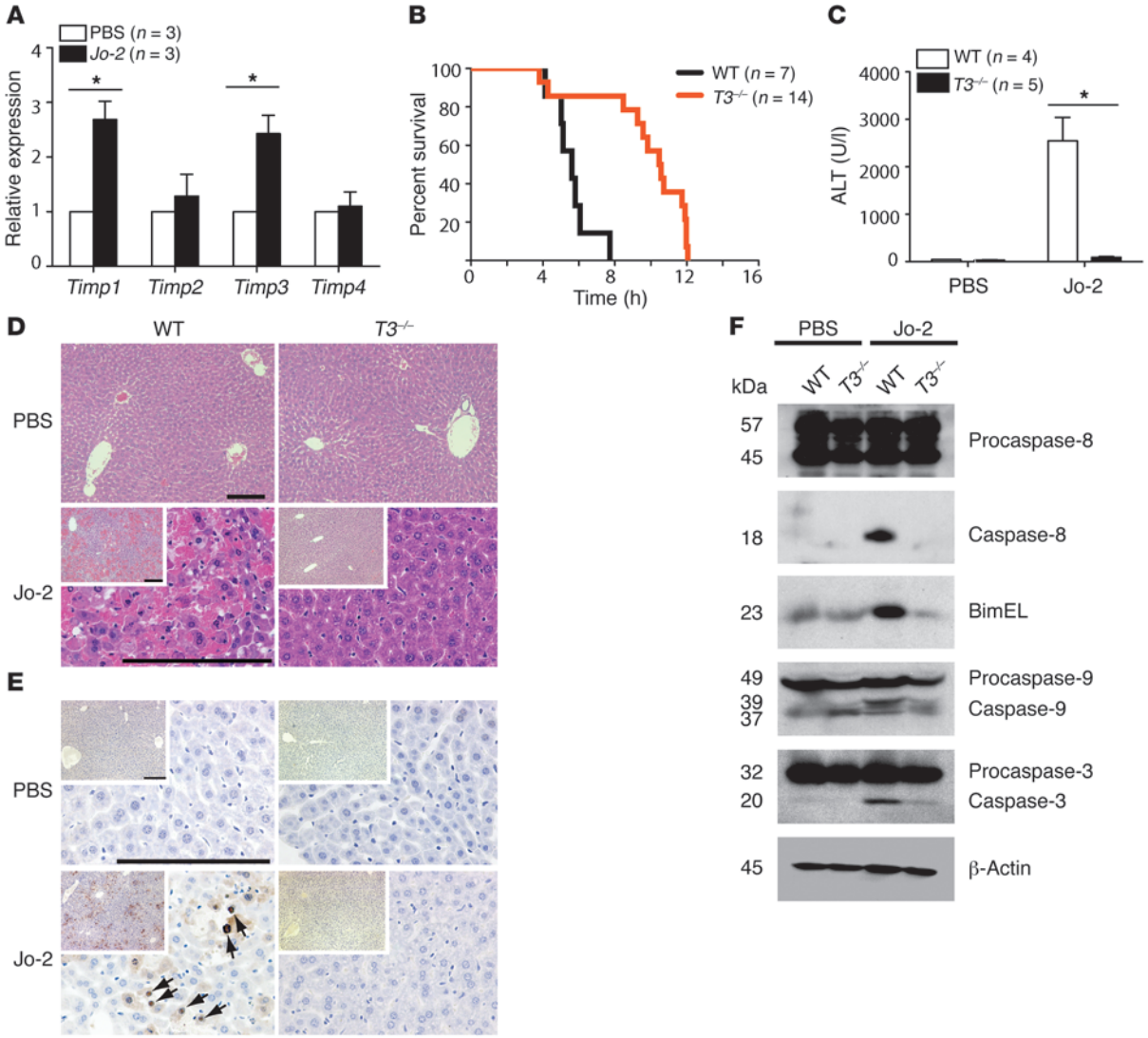

Figure 2

Delay of Fas-mediated apoptosis and hepatotoxicity in *Timp3*$^{-/-}$ mice. (**A**) qRT-PCR analysis of *Timp1*, *Timp2*, *Timp3*, and *Timp4* mRNA shows elevated expression of *Timp1* and *Timp3* in livers of wild-type mice treated with 0.65 μg/g Jo-2. Liver mRNA was obtained 3 hours after injection. *$P < 0.05$. Data are mean ± SEM ($n = 3$). (**B**) Survival curve of WT and *Timp3*$^{-/-}$ (*T3*$^{-/-}$) mice treated with 0.65 μg/g Jo-2. $P < 0.005$ versus WT (log-rank test). (**C**–**F**) WT and *T3*$^{-/-}$ mice were treated with PBS or 0.65 μg/g Jo-2. Three hours after injection, mice were sacrificed to obtain liver and serum. (**C**) Hepatotoxicity measured by serum ALT levels in WT and *T3*$^{-/-}$ mice. *$P < 0.05$. Data are mean ± SEM ($n = 4$). (**D**) Histology (H&E) of WT (from Figure 1C) and *T3*$^{-/-}$ livers 3 hours after treatment with PBS or Jo-2 reveals absence of tissue damage, hemorrhaging, and apoptotic bodies in *T3*$^{-/-}$ liver. Scale bars: 100 μm. (**E**) Immunohistochemical staining of active caspase-3 (arrows). *T3*$^{-/-}$ liver exhibits lack of caspase-3 activation. Sections are representative of at least 4 mice per genotype and treatment. Scale bars: 100 μm. (**F**) Immunoblot analysis of caspase-8, -9, and -3 processing and BimEL induction in liver lysates. All data are representative of at least 3 independent experiments.

Results

TNF signaling sensitizes hepatocytes to Fas-mediated apoptosis. The liver is highly sensitive to inflammatory and apoptotic stimuli of TNF superfamily members such as Fas, TNF, and TRAIL (1, 7); however, the exact role of TNF signaling in mouse models of Fas-mediated hepatotoxicity has yet to be defined. Primary murine hepatocytes were tested for their sensitivity to Fas-mediated apoptosis in the presence of a low level of TNF (1 ng/ml). TNF enhanced apoptosis in wild-type hepatocyte cultures treated with the Fas agonist Jo-2, as measured by caspase-3/7 activity. However, TNF on its own was not cytotoxic at this low concentration (Figure 1A). This highlights the potency of TNF in promoting Fas-mediated apoptosis.

While mice lacking *Tnfr1* have previously demonstrated sensitivity to Fas-mediated hepatotoxicity (24), the kinetics of their survival has not been explored. Here we utilized a clone of Jo-2 (listed in Methods) that allowed us to dissect the kinetics of survival after induction of hepatotoxicity. Wild-type, *Tnf*-deficient (*Tnf*$^{-/-}$), and *Tnfrsf1a*-deficient (*Tnfr1*$^{-/-}$) mice received a lethal dose of Jo-2 (0.65 μg/g i.p.). Both knockouts showed a significant delay in fulminant hepatic failure, with a time to morbidity of approximately 10 hours compared with 5 hours for wild-type controls (Figure 1B).

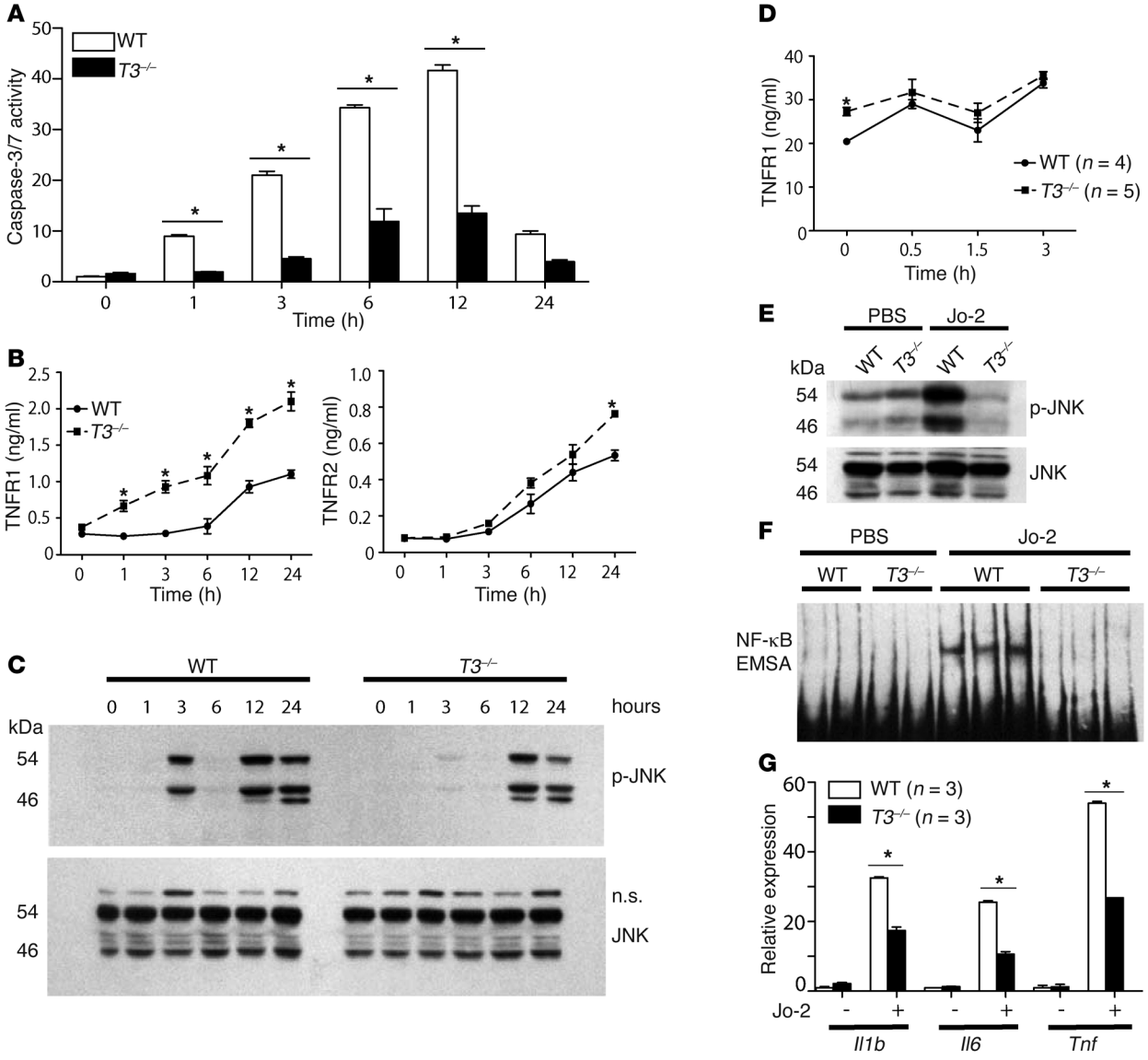

Figure 3

Decreased hepatocyte apoptosis correlates with enhanced TNFR1 shedding and abrogated TNF signaling upon loss of *Timp3*. (**A**) Twenty-four-hour time course of apoptosis measured by caspase-3/7 activity in WT and *T3*$^{-/-}$ primary hepatocytes treated with 1 ng/ml TNF and 10 ng/ml Jo-2. *$P < 0.03$. Data are mean ± SD ($n = 3$). (**B**) ELISA of TNFR1 and TNFR2 release into hepatocyte culture media from **A**. *$P < 0.002$ versus WT. Data are mean ± SD ($n = 3$). (**C**) Immunoblots of JNK phosphorylation in hepatocyte lysates from **A**. n.s., nonspecific. (**D**) ELISA of serum TNFR1 levels in WT and *T3*$^{-/-}$ mice before (0 hours) and after 0.65 μg/g Jo-2 treatment. *$P = 0.003$. Data are mean ± SEM ($n = 4$). (**E**) Immunoblots of JNK phosphorylation in liver lysates from WT and *T3*$^{-/-}$ mice 3 hours after treatment with PBS or 0.65 μg/g Jo-2. (**F**) NF-κB binding activity was assayed in nuclear lysates of WT and *T3*$^{-/-}$ mouse livers from **E** using EMSA. (**G**) qRT-PCR analysis of proinflammatory cytokine mRNA levels in WT and *T3*$^{-/-}$ livers from **E**. *$P < 0.01$. Data are mean ± SEM ($n = 3$). All data are representative of at least 2 independent experiments.

An in vitro time course of hepatocyte apoptosis over 24 hours using 1 ng/ml TNF plus 10 ng/ml Jo-2 revealed comparable caspase-3/7 activation in *Tnf*$^{-/-}$ and wild-type cells as expected when exogenous TNF was added to culture, whereas *Tnfr1*$^{-/-}$ hepatocytes exhibited decreased caspase-3/7 activation (Supplemental Figure 1A; supplemental material available online with this article; doi:10.1172/JCI42686DS1). Histological examination of livers 3 hours after administration of PBS (vehicle) or Jo-2 revealed extensive tissue damage and hemorrhaging only in the wild-type mice; however, mice of all genotypes eventually succumbed to fulminant hepatic failure with similar liver damage (Figure 1C and Supplemental Figure 5). Immunohistochemical staining revealed activation of caspase-3 only in wild-type livers after Jo-2 administration (Figure 1C). Serum alanine transaminase (ALT), a marker of hepatotoxicity, was significantly elevated in wild-type mice 3 hours after Jo-2 administration (Figure 1D). Further, processing of caspase-8 and -3 was seen in wild-type liver lysates, indicating the onset of apoptosis in these mice (Figure 1E). In contrast, *Tnf*$^{-/-}$ and *Tnfr1*$^{-/-}$ mice exhibited lower serum ALT and a lack of caspase activation, revealing that TNF signaling sensitizes to fulminant hepatitis in vivo.

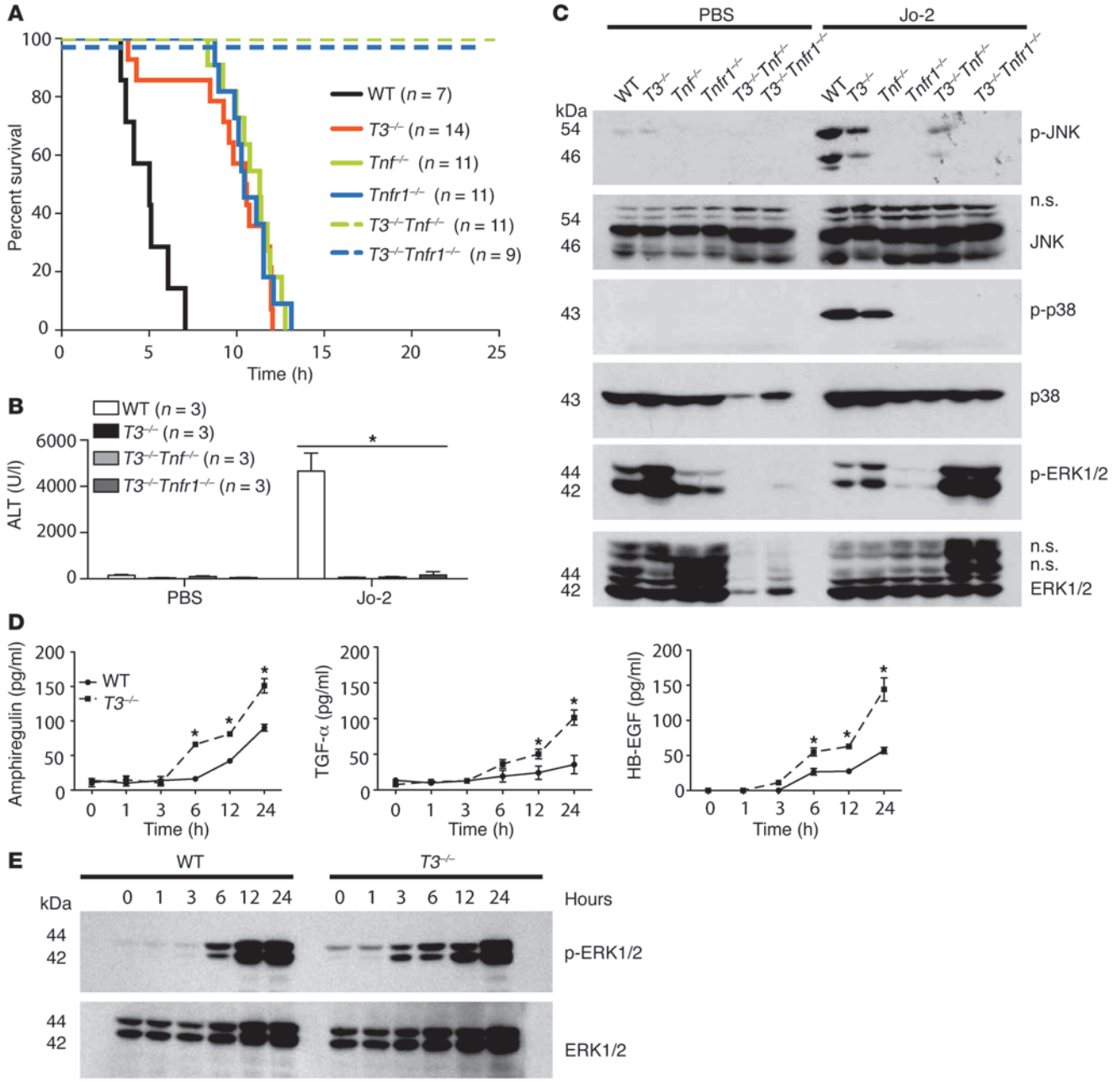

Figure 4

Compound loss of *Timp3* and *Tnf* or *Tnfr1* completely prevents Fas-mediated hepatotoxicity and reveals accelerated ERK1/2 phosphorylation. (**A**) Survival curve of WT, *T3*$^{-/-}$*Tnf*$^{-/-}$, and *T3*$^{-/-}$*Tnfr1*$^{-/-}$ compound knockout mice (dashed lines) treated with 0.65 μg/g Jo-2, superimposed on survival curves of *T3*$^{-/-}$, *Tnf* $^{-/-}$, and *Tnfr1*$^{-/-}$ mice from Figure 1B and Figure 2B. (**B**) Hepatotoxicity measured by serum ALT levels in mice of indicated genotypes 3 hours after treatment with PBS or Jo-2. *$P < 0.05$. Data are mean ± SEM ($n = 3$). (**C**) Immunoblots of JNK and ERK1/2 phosphorylation in liver lysates of indicated genotypes 3 hours after treatment with PBS or Jo-2. (**D**) ELISA of amphiregulin, HB-EGF, and TGF-α released by WT and *T3*$^{-/-}$ hepatocytes treated with 1 ng/ml TNF plus 10 ng/ml Jo-2 over 24 hours. *$P = 0.02$ versus WT. Data are mean ± SD ($n = 3$). (**E**) Immunoblots of ERK1/2 phosphorylation in hepatocyte lysates from **C**. Data in **B**, **D**, and **E** are representative of at least 2 independent experiments.

Delay of Fas-induced apoptosis in Timp3$^{-/-}$ *livers*. A hallmark of fulminant hepatic failure, often lethal in the clinical setting, is the rapid induction of hepatocyte apoptosis (25). Metalloproteinases and their inhibitors may orchestrate the onset of acute tissue damage by regulating cytokine bioavailability in the microenvironment. Thus, hepatic expression of selected *Timp*, *Adam*, and *Mmp* genes was assayed using quantitative RT-PCR (qRT-PCR) following administration of Jo-2 to wild-type mice. *Timp1* and *Timp3*, but not *Timp2* or *Timp4*, were significantly upregulated subsequent to Jo-2 injection (Figure 2A). Of the *Adam* (*Adam9*, *-10*, *-12*, *-17*) and *Mmp* (*Mmp2*, *-9*, and *-14*) genes evaluated, *Adam12* and *Mmp2* expression changed upon Jo-2 administration, but the rest remained com-

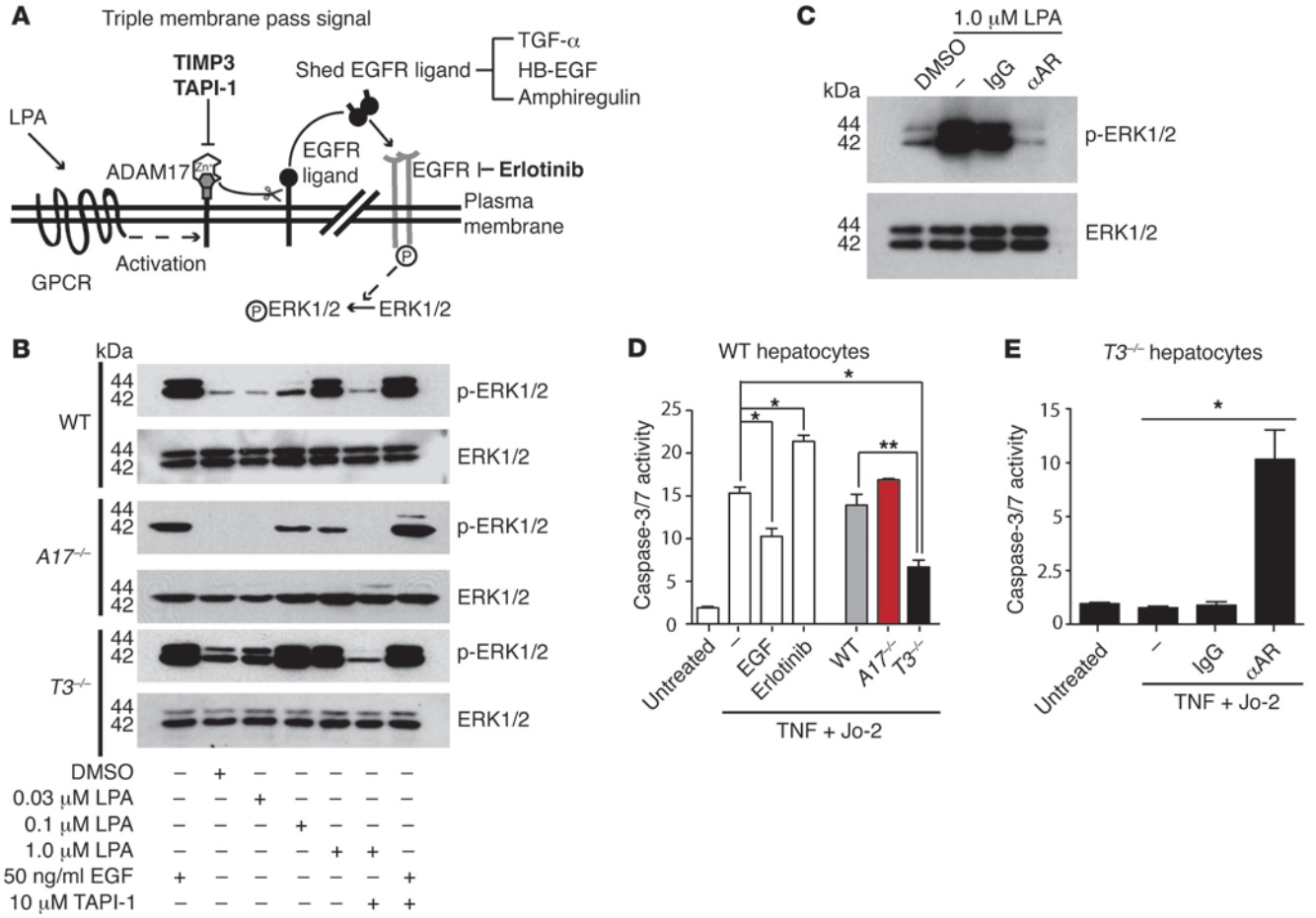

Figure 5

Loss of *Timp3* enhances hepatoprotective EGFR ligand shedding and downstream ERK1/2 phosphorylation. (**A**) Schematic of LPA-induced EGFR signaling via the "triple membrane pass signal" mechanism. (**B**) Immunoblots assaying ERK1/2 phosphorylation in MEFs of the indicated genotypes treated with listed doses of LPA. TAPI-1 is an ADAM inhibitor; soluble EGF was used as a positive control. WT and *T3*$^{-/-}$ immunoblots are representative of at least two independently derived primary MEF lines from different embryos. *A17*$^{-/-}$, *ADAM17*$^{-/-}$. (**C**) *T3*$^{-/-}$ MEFs were pretreated with 5.0 μg/ml IgG or αAR 2 hours prior to treatment with 1.0 μM LPA for 5 minutes, and ERK1/2 phosphorylation was subsequently assayed. (**D**) Wild-type hepatocytes were pretreated for 3 hours with conditioned media from LPA-treated MEFs of the indicated genotypes (colored bars), then treated with 1 ng/ml TNF plus 10 ng/ml Jo-2 for an additional 3 hours. As controls, hepatocytes were left untreated or pretreated with EGF or with erlotinib (white bars). *P < 0.01 versus TNF + Jo-2–treated hepatocytes that were not pretreated; **P = 0.004. Data are mean ± SD (n = 3). (**E**) *T3*$^{-/-}$ hepatocytes were pretreated with 5.0 μg/ml IgG or αAR for 3 hours prior to treatment with TNF + Jo-2 as in **D**. *P < 0.001 versus no pretreatment. Data are mean ± SD (n = 3). All data are representative of at least 2 independent experiments.

parable in PBS- and Jo-2–treated mice (Supplemental Figure 1B). *Timp3*$^{-/-}$ mice have increased TNF bioactivity in other models of hepatic inflammation (22, 23, 26); we thus hypothesized that they would also display enhanced susceptibility to Jo-2. Surprisingly, *Timp3*$^{-/-}$ mice exhibited a resistance similar to that observed in *Tnf*$^{-/-}$ and *Tnfr1*$^{-/-}$ mice and survived significantly longer than wild-type controls after Jo-2 administration (Figure 2B, P = 0.005, log-rank test). Negligible serum ALT and the absence of tissue damage (H&E) 3 hours after Jo-2 administration confirmed diminished hepatotoxicity in *Timp3*$^{-/-}$ mice (Figure 2, C and D).

Hepatocytes utilize the intrinsic pathway of apoptosis, requiring a loss of mitochondrial membrane potential induced by proapoptotic members of the Bcl-2 family prior to activation of downstream caspase-9 and -3 (1, 5). Immunohistochemical staining revealed widespread caspase-3 activation in wild-type but not *Timp3*$^{-/-}$ livers at this time point (Figure 2E). Processing of caspase-8 and -9 was also found to be absent in *Timp3*$^{-/-}$ livers (Figure 2F), and additionally the elevation in Bim supported activation of intrinsic apoptosis only in wild-type livers (Figure 2F). Fluorogenic caspase-3 and -9 activity assays confirmed their functional activation in wild-type mice (Supplemental Figure 1C). A potential mechanism explaining the dampened proapoptotic response in *Timp3*$^{-/-}$ livers could be altered expression and shedding of Fas itself. Immunoblots of liver lysates from wild-type and *Timp3*$^{-/-}$ mice treated with PBS or Jo-2 revealed no differences in Fas protein expression. Additionally, flow cytometry analysis of cell surface expression on untreated hepatocytes showed comparable levels of Fas in wild-type and *Timp3*$^{-/-}$ mice (Supplemental Figure 2). These findings indicate that the hepatoprotection observed in *Timp3*$^{-/-}$ mice is not likely due to changes in Fas levels. Overall, diminished caspase activation and a lack of BimEL induction demonstrated delayed hepatocyte apoptosis in Jo-2–treated mice lacking *Timp3*.

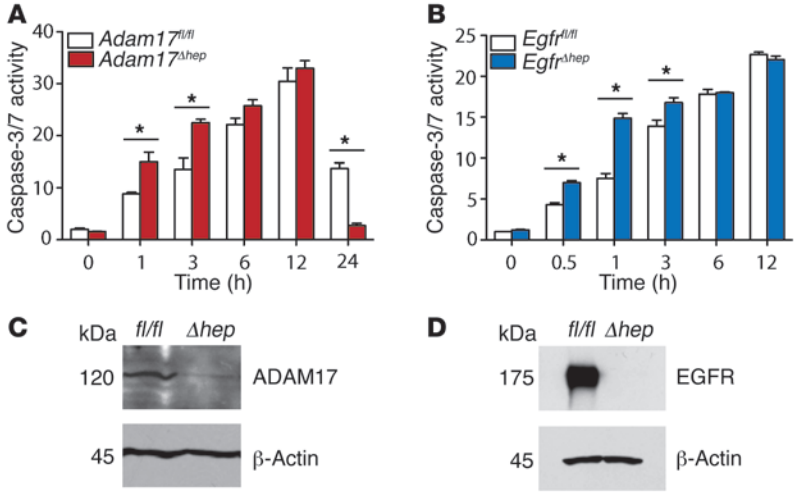

Figure 6
ADAM17 and EGFR are individually hepatoprotective against Fas-mediated hepatotoxicity. (**A**) Apoptosis time course of control (*Adam17*$^{fl/fl}$) or *Adam17*-deficient (*Adam*$^{\Delta hep}$) hepatocytes treated with 1 ng/ml TNF plus 10 ng/ml Jo-2, measured by caspase-3/7 activity. (**B**) Control (*Adam17*$^{fl/fl}$) or *Egfr*-deficient (*Adam*$^{\Delta hep}$) hepatocytes were treated as in **A**, and apoptosis was measured by caspase-3/7 activity. *$P < 0.04$. Data are mean ± SD ($n = 3$). Apoptosis time course of both mutants was repeated in an independent experiment, with consistent results. (**C** and **D**) Confirmation of *Adam17* and *Egfr* deletion by immunoblot.

TNFR1 shedding dampens JNK phosphorylation and NF-κB activation in Timp3$^{-/-}$ *liver*. We next asked whether the kinetics of apoptosis and TNF signal transduction were altered in a TIMP3-deficient state. A 24-hour apoptosis time course of wild-type and *Timp3*$^{-/-}$ hepatocyte cultures treated with 1 ng/ml TNF plus 10 ng/ml Jo-2 showed significantly less caspase-3/7 activity in *Timp3*$^{-/-}$ cells across all time points (Figure 3A). Poly-ADP ribose polymerase (PARP) is a physiological target of activated caspase-3; significantly greater PARP cleavage was observed from 3 to 12 hours in wild-type hepatocytes compared with *Timp3*$^{-/-}$ cells treated with TNF plus Jo-2 (Supplemental Figure 3A). Of the two TNFRs, TNFR1 associates with TRADD and FADD to initiate caspase activation, and we thus asked whether the transient hepatoprotection observed in the absence of TIMP3 correlated with TNFR shedding. ELISA specific to the extracellular domains of TNFR1 and TNFR2 in hepatocyte culture media over the 24-hour apoptosis time course showed significantly greater TNFR1 release by *Timp3*$^{-/-}$ compared with wild-type hepatocytes but only modest release of TNFR2 (Figure 3B). Fas and Fas ligand were undetectable in hepatocyte culture media as well as in mouse serum across all treatments in both genotypes (data not shown). Activation of the stress kinase JNK is an important component of TNFR signaling during stress response. Phosphorylated JNK promotes intrinsic apoptosis by activating the proapoptotic BH3-only protein Bim and degrading antiapoptotic Mcl-1 (1, 7, 27–29). In accordance with elevated TNFR1 shedding, early JNK phosphorylation was ablated in *Timp3*$^{-/-}$ hepatocytes 3 hours after treatment, although it was comparable at 12 and 24 hours (Figure 3C). JNK phosphorylation is known to occur in transient and prolonged phases, with each having distinct consequences for cell survival (30–32). Here we see that loss of *Timp3* ablates the early transient phase while maintaining prolonged activation. Next, in vivo analysis of TNFR1 and -2 shedding and JNK phosphorylation was performed. Constitutively higher serum levels of TNFR1 (Figure 3D) but not TNFR2 (data not shown) were seen in *Timp3*$^{-/-}$ mice, along with diminished JNK phosphorylation in *Timp3*$^{-/-}$ livers 3 hours after Jo-2 injection (Figure 3E). These data indicate that loss of *Timp3* increased TNFR1 shedding and dampened early stress kinase activation in vitro and in vivo.

In addition to phosphorylation of the stress kinases, NF-κB activation downstream of TNFR1 is observed in numerous models of hepatotoxicity (33, 34). EMSA detected active NF-κB in hepatic nuclear fractions of wild-type mice treated with Jo-2, but not mice lacking TIMP3 (Figure 3F). Consistent with this, significantly higher induction of proinflammatory target genes *Il1b*, *Il6*, and *Tnf* was observed in wild-type livers compared with *Timp3*$^{-/-}$ tissue (Figure 3G). We also measured hepatic *Tnfrsf1a* (*Tnfr1*) and *Tnfrsf1b* (*Tnfr2*) expression, which were comparable across both genotypes before and after Jo-2 treatment (Supplemental Figure 3B). Basal *Adam17* expression measured by qRT-PCR was found to be higher in *Timp3*$^{-/-}$ liver, as we have previously reported (22) (Supplemental Figure 3B). Together, the data indicate that TIMP3 deficiency ablated TNF signaling in response to hepatic death receptor activation, as made apparent by diminished JNK phosphorylation and NF-κB activity. Further, this abrogation was not due to reduced expression of TNFRs but arose from increased ectodomain shedding of TNFR1.

Signaling through AKT or AMPKβ does not contribute to hepatoprotection in Timp3$^{-/-}$ *mice*. Prosurvival signaling through AKT is reported to inhibit Mcl-1 degradation by GSK3β and JNK1/2 (29, 35). We therefore assayed AKT phosphorylation upon treatment with Jo-2. AKT phosphorylation was comparable in wild-type and *Timp3*$^{-/-}$ livers treated with and without Jo-2, implying that AKT activation during Fas-induced hepatotoxicity does not contribute to the survival of *Timp3*$^{-/-}$ mice (Supplemental Figure 4A). Metabolic stress in hepatocytes is known to exacerbate tissue response to proinflammatory or cytotoxic insult (26); however, AMPKβ phosphorylation was also comparable in wild-type and *Timp3*$^{-/-}$ liver lysates after Jo-2 treatment (Supplemental Figure 4B). Altered lipid metabolism through AMPK signaling probably did not account for the resistance observed in *Timp3*$^{-/-}$ mice.

Compound deletions of Timp3/Tnf or Timp3/Tnfr1 completely prevent hepatic failure and involve enhanced ERK1/2 phosphorylation. To investigate whether decreased TNF signaling was the primary mechanism promoting the survival of *Timp3*$^{-/-}$ mice following Fas-mediated hepatotoxicity, we bred *Timp3*$^{-/-}$ mice with *Tnf*$^{-/-}$ and *Tnfr1*$^{-/-}$ mice. Remarkably, both strains of double knockout mice were completely resistant to the lethal dose of Jo-2 (Figure 4A); histological analysis showed that the *Timp3*$^{-/-}$*Tnf*$^{-/-}$ and *Timp3*$^{-/-}$*Tnfr1*$^{-/-}$ compound knockouts exhibited little evidence of tissue damage even at 24 hours (Supplemental Figure 5). Analysis of serum ALT verified a lack of hepatotoxicity in *Timp3*$^{-/-}$*Tnf*$^{-/-}$ and *Timp3*$^{-/-}$*Tnfr1*$^{-/-}$ compound knockouts 3 hours after Jo-2 treatment when compared with wild-type mice (Figure 4B). This implied the involvement of additional, parallel signals relevant to hepatocyte survival that may be regulated by TIMP3.

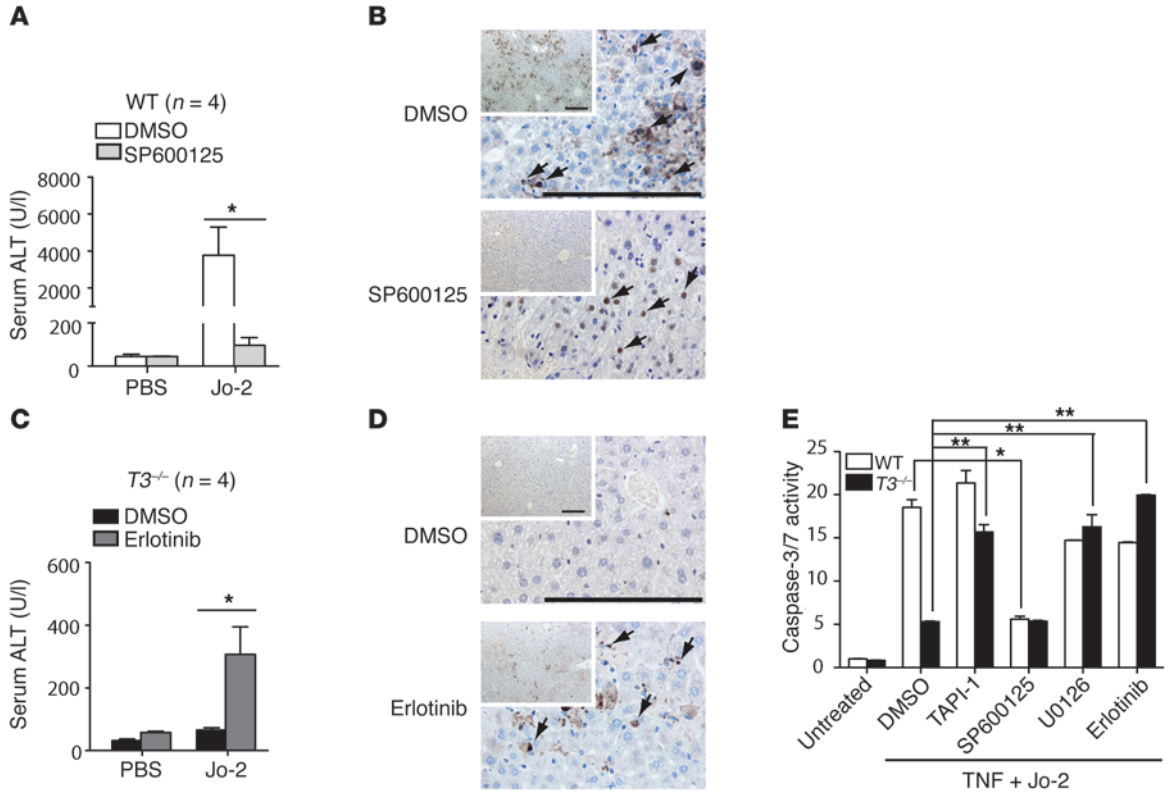

Figure 7

TIMP3 is an upstream regulator of EGFR and MAPK activity in Fas-induced hepatotoxicity. (**A**) Serum ALT measurements of WT mice pretreated with the JNK inhibitor SP600125 or vehicle (PBS + 10% DMSO) 45 minutes prior to Jo-2 or PBS treatment. *$P < 0.05$. Data are mean ± SEM ($n = 4$). (**B**) Immunohistochemistry depicting active caspase-3 (arrows) only in WT livers of mice pretreated with DMSO prior to Jo-2 administration. Scale bars: 100 μm. (**C**) Serum ALT measurements of *T3*$^{-/-}$ mice pretreated with erlotinib or vehicle 1 hour prior to Jo-2 or PBS treatment. *$P < 0.05$. Data are mean ± SEM ($n = 4$). (**D**) Immunohistochemistry depicting active caspase-3 (arrows) in *T3*$^{-/-}$ livers pretreated with EGFR inhibitor erlotinib. Scale bars: 100 μm. (**E**) Hepatocytes were treated with vehicle only (DMSO), inhibitors of ADAM17 (TAPI-1), JNK (SP600125), ERK1/2 kinase MEKK (U0126), EGFR (erlotinib) for 1 hour, followed by addition of TNF plus Jo-2 for 3 hours. Apoptosis was measured as caspase-3/7 activity. *$P = 0.0002$, **$P < 0.002$ versus DMSO. Data are mean ± SD ($n = 3$). Data are representative of at least 2 independent experiments.

Given the known activation of MAPKs during the cytokine-induced stress response, we assessed JNK, p38, and ERK1/2 phosphorylation in livers of all 6 genotypes with or without Jo-2 injection. Loss of either *Tnf* or *Tnfr1* per se eliminated JNK and p38 phosphorylation in response to Jo-2, confirming the importance of TNF signaling via stress-activated protein kinases in Fas-mediated hepatotoxicity (Figure 4C). TIMP3 deficiency did not significantly affect p38 phosphorylation, ruling out a role for this MAPK in resistance to Fas-mediated hepatotoxicity in *Timp3*$^{-/-}$ mice (Figure 4C). In contrast, constitutive ERK1/2 phosphorylation was markedly elevated in untreated livers of *Timp3*$^{-/-}$ mice compared with other genotypes (Figure 4C). After Jo-2 treatment, ERK1/2 phosphorylation was greater in the double knockout livers compared with other genotypes. Collectively, these data indicate that TIMP3 deficiency activates pathways upstream of ERK1/2, potentially providing hepatoprotection.

In addition to TNF and its receptors, EGFR ligands (HB-EGF, TGF-α, amphiregulin) are critical substrates of ADAM17, which is inhibited by TIMP3 (18, 36, 37). *Adam17*$^{-/-}$ mice phenocopy *Egfr*$^{-/-}$ mice, and hepatic deletion of *Egfr* results in failed liver regeneration, indicating its requirement as a mitogenic stimulus for hepatocyte division (38). We therefore analyzed EGFR signaling in wild-type and *Timp3*$^{-/-}$ primary hepatocytes. ELISA was used to measure the shedding of the EGFR ligands amphiregulin, HB-EGF, and TGF-α into media over a 24-hour time course of TNF plus Jo-2 treatment. Significantly elevated concentrations of all 3 ligands were found in *Timp3*$^{-/-}$ hepatocyte culture media (Figure 4D). Consistent with higher EGFR ligand release, *Timp3*$^{-/-}$ hepatocytes showed accelerated ERK1/2 phosphorylation (Figure 4E). These data suggest that enhanced release of multiple EGFR ligands was responsible for increased EGFR phosphorylation, which in turn activated survival signals through ERK1/2, contributing to the observed resistance of *Timp3*$^{-/-}$ mice to Fas-mediated hepatotoxicity.

TIMP3 inhibits metalloproteinase-dependent EGFR signaling. Of the 4 proteins encoded by *Timp* genes, only TIMP3 physiologically inhibits ADAM17 activity (22, 37), and we reasoned that EGFR signaling would be checked by TIMP3. We utilized a previously established assay to measure GPCR-mediated EGFR signaling in a metalloproteinase-dependent manner (10, 17, 39, 40) as shown in the schematic (Figure 5A). Mouse embryonic fibroblasts (MEFs) were stimulated with oleoyl-L-α-lysophosphatidic acid sodium salt (LPA; a GPCR agonist), and the response was assayed by immunoblotting for phosphorylated EGFR and ERK1/2. Wild-type MEFs showed increasing ERK1/2 phosphorylation in a dose-dependant manner, while MEFs lacking *Adam17* showed diminished ERK1/2 phos-

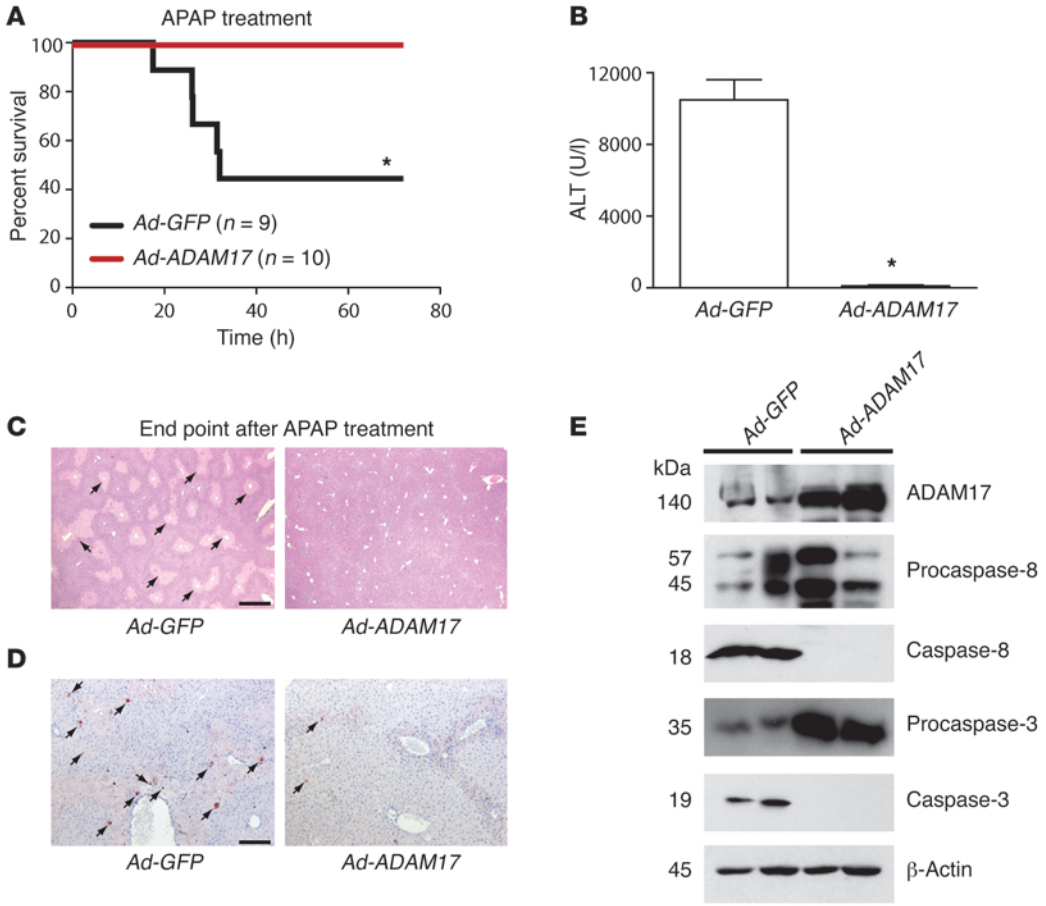

Figure 8

Ectopic ADAM17 delivery protects against APAP-driven fulminant hepatitis. (**A**) Survival of wild-type mice expressing hepatic *Adam17* or *Gfp* after treatment with a lethal dose of APAP. Adenoviral ADAM17 (*Ad-ADAM17*) or GFP (*Ad-GFP*) was injected intravenously into wild-type mice 96 hours prior to treatment with 600 mg/kg APAP. Survival was followed for the next 72 hours. **P* = 0.013 versus Ad-GFP (log-rank test). (**B**) Hepatotoxicity measured by serum ALT levels from mice treated as in **A**. **P* < 0.01. Data are mean ± SEM (*n* = 3). (**C**) Histological analysis of liver damage at the survival endpoints. Significant necrosis is observed only in *Ad-GFP* livers (arrows). Images are representative of at least 5 mice. Scale bar: 100 μm. (**D**) Immunohistochemical staining of active caspase-3 (arrows) shows induction of apoptosis in *Ad-GFP* livers after APAP treatment. Images are representative of 3 mice per group. Scale bar: 100 μm. (**E**) Immunoblots of ADAM17 in liver lysates confirming delivery of adenoviral ADAM17 to the liver. Immunoblots for cleaved caspase-8 and -3 depict onset of APAP-induced apoptosis in *Ad-GFP* mice.

phorylation under the same treatment conditions. On the other hand, loss of *Timp3* resulted in markedly enhanced ERK1/2 phosphorylation (Figure 5B). Phosphorylated ERK1/2 was also seen in the absence of LPA in TIMP3-deficient MEFs. As controls in this series of experiments, pretreatment of all MEFs with the small molecule ADAM inhibitor TNF-α protease inhibitor–1 (TAPI-1) abolished ERK1/2 phosphorylation at the highest dose of LPA, while soluble EGF bypassed the requirement of metalloproteinase activity. Sustained EGFR phosphorylation in *Timp3*$^{-/-}$ MEFs confirmed enhanced signaling owing to elevated metalloproteinase activity (Supplemental Figure 6A). We next tested whether shed EGFR ligands are relevant to receptor activation through antibody-mediated depletion in culture media. Given that commercial availability of a murine-specific neutralizing antibody was limited to amphiregulin, *Timp3*$^{-/-}$ MEFs were stimulated with LPA in the presence of neutralizing amphiregulin antibody (αAR). Indeed, pretreatment with this antibody significantly diminished ERK1/2 phosphorylation, indicating that soluble amphiregulin contributed to EGFR signaling (Figure 5C). Thus, TIMP3 is a specific negative regulator of metalloproteinase-dependent EGFR signaling.

Increased EGFR ligand shedding is hepatoprotective. We next asked whether enhanced hepatic EGFR signaling due to increased ligand bioavailability was directly protective against Fas-induced cell death. Conditioned media was collected from wild-type, *Adam17*$^{-/-}$, and *Timp3*$^{-/-}$ MEFs stimulated with LPA and subsequently added to wild-type hepatocytes treated with Jo-2 plus TNF (Figure 5D). As independent controls, hepatocytes were pretreated with EGF for protection or with erlotinib (an EGFR receptor tyrosine kinase inhibitor) for sensitization to apoptosis (Figure 5D). Conditioned media from *Timp3*$^{-/-}$ MEFs provided hepatoprotection, whereas other genotypes had no effect. Since we had observed that shed amphiregulin plays a functional role in EGFR signaling, we tested whether neutralizing soluble amphiregulin would resensitize *Timp3*$^{-/-}$ hepatocytes to apoptosis. We observed far greater caspase-3/7 activation upon addition of αAR during TNF plus Jo-2 treatment of *Timp3*$^{-/-}$ hepatocytes (Figure 5E). A physiological conse-

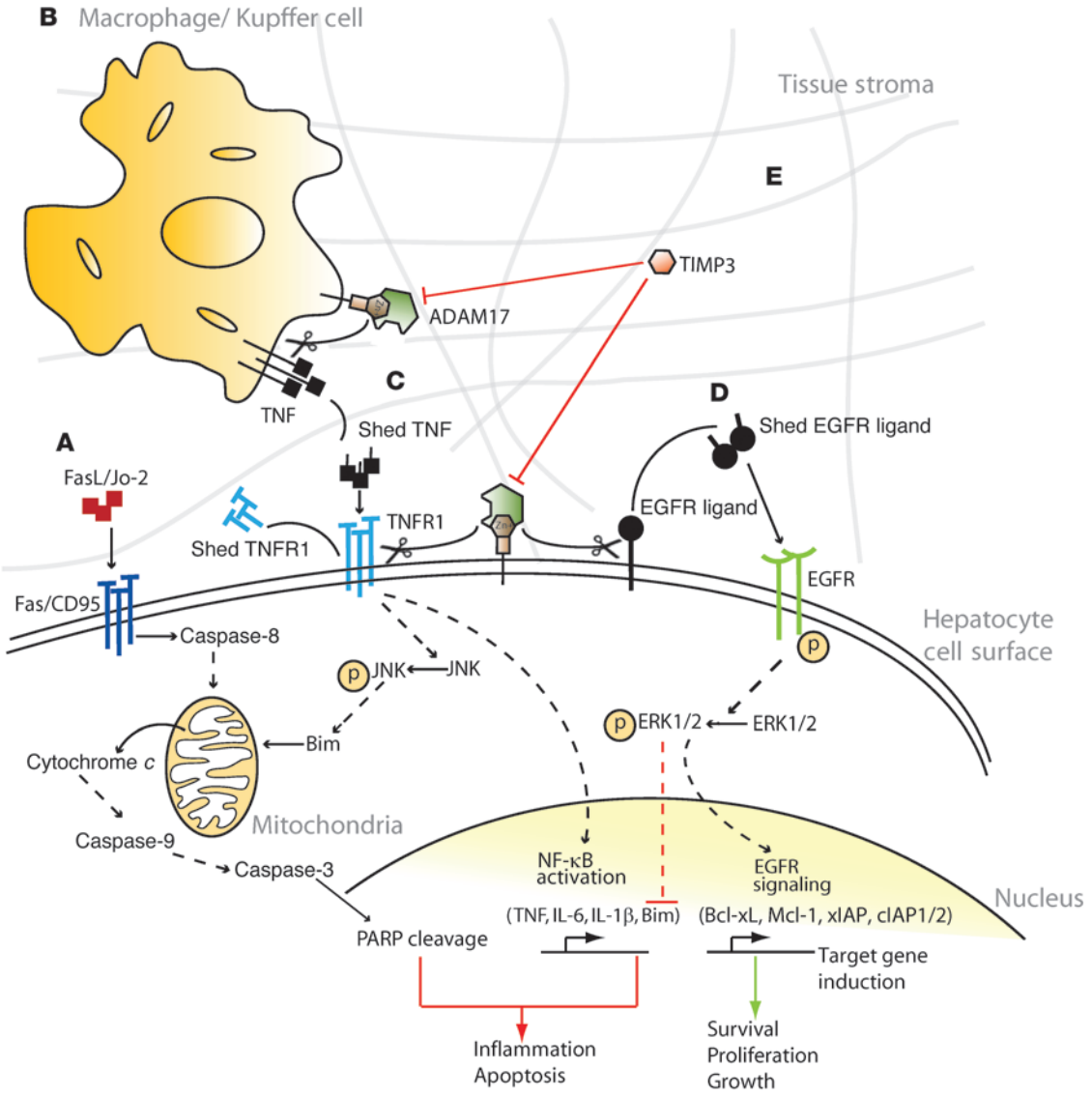

Figure 9

Inhibition of cell surface ADAM17 impacts MAPKs during stress responses and provides stromal regulation of cell survival. (**A**) Fas activation triggers intrinsic apoptosis. (**B**) Macrophage (Kupffer cell) activation results in TNF shedding, which acts as a secondary sensitizer to Fas-mediated toxicity. (**C**) TNF/TNFR1 binding activates both stress kinases (JNK) and NF-κB. ADAM17 shedding of TNFR1 dampens proapoptotic signaling. (**D**) ADAM17 shedding of EGFR ligands provides protection from apoptosis through ERK1/2 signaling. (**E**) The hepatic microenvironment harbors TIMP3, which checks ADAM17 activity.

quence of EGFR ligand availability during acute stress is induction of EGFR signaling and subsequent transcription of antiapoptotic genes or suppression of proapoptotic signals. Bcl family members *Mcl1* and *Bcl-xL* (*Bcl2l1*), along with *Xiap* and *Ciap1/2* (*Birc3*), are putative EGFR targets (41–43), and we observed that loss of *Timp3* resulted in elevated transcription of these prosurvival genes upon Jo-2 treatment (Supplemental Figure 6B). Additionally, MAPK activation downstream of EGFR is known to antagonize *Bim* transcription. Consistent with this, we observed that *Timp3*$^{-/-}$ livers exhibited decreased BimEL levels upon Jo-2 treatment (Figure 2F). Therefore, TIMP3 deficiency enhances ectodomain shedding of EGFR ligands, among which amphiregulin is a significant contributor to hepatoprotection against death receptor activation.

Hepatocyte-specific loss of ADAM17 or EGFR promotes Fas-induced killing. In order to directly determine the role of ADAM17 and EGFR in Fas-mediated hepatocyte apoptosis, we generated mice that lack ADAM17 or EGFR in hepatocytes by crossing *Adam17*$^{fl/fl}$ or *Egfr*$^{fl/fl}$ mice with those expressing *Cre* recombinase under control of the albumin promoter. Primary hepatocyte cultures were generated from control (*Adam17*$^{fl/fl}$, *Egfr*$^{fl/fl}$) and hepatocyte-specific knockout mice (*Adam17*$^{\Delta hep}$, *Egfr*$^{\Delta hep}$, respectively). Significantly elevated caspase-3/7 activation was observed in *Adam17*$^{\Delta hep}$ hepatocytes at 1 and 3 hours after TNF plus Jo-2 treatment (Figure 6A). Additionally, TNFR1, amphiregulin, HB-EGF, and TGFα levels were undetectable over the time course in *Adam17*$^{\Delta hep}$ culture media (data not shown). As with *Adam17*$^{\Delta hep}$ cells, *Egfr*$^{\Delta hep}$ hepatocytes exhibited increased caspase-3/7

activity at early time points compared with *Egfr*$^{fl/fl}$ controls (Figure 6B). To confirm the protective role of ADAM17 in vivo, we injected *Adam17*$^{\Delta hep}$ and *Adam17*$^{fl/fl}$ control mice with a lower dose of Jo-2 (0.33 μg/g) and monitored for survival over 3 days after treatment. A greater fraction of *Adam17*$^{\Delta hep}$ mice died within 3 days compared with *Adam17*$^{fl/fl}$ mice (5 of 7 *Adam17*$^{\Delta hep}$ mice versus 2 of 5 *Adam17*$^{fl/fl}$ mice). *Cre*-mediated deletion of ADAM17 or EGFR in hepatocytes was validated via immunoblotting (Figure 6, C and D, respectively). We conclude that ADAM17 and EGFR individually provide hepatoprotection against Fas-induced killing.

Inhibitors of MAPK, EGFR, or ADAM17 reverse the Timp3$^{-/-}$ *resistance to Fas*. To confirm that TIMP3 is functionally upstream of JNK and ERK1/2 signal transduction pathways, we first examined the in vivo consequence of MAPK inhibition on hepatotoxicity. Pretreatment of wild-type mice with a JNK inhibitor (SP600125) led to decreased serum ALT and hepatic caspase-3 activation versus those treated with vehicle (Figure 7, A and B). On the other hand, *Timp3*$^{-/-}$ mice pretreated with an EGFR inhibitor (erlotinib) exhibited elevated serum ALT and hepatic caspase-3 activation upon Jo-2 injection compared with those pretreated with vehicle (Figure 7, C and D). Next, small molecule inhibitors of ADAM17 (TAPI-1), JNK (SP600125), ERK1/2 kinase MEKK (U0126), and EGFR (erlotinib) were added to wild-type and *Timp3*$^{-/-}$ hepatocyte cultures treated with TNF plus Jo-2 for 3 hours. The inhibition of ADAM17, ERK1/2, or EGFR activity in *Timp3*$^{-/-}$ hepatocytes significantly elevated caspase-3/7 activity, while JNK inhibition in wild-type hepatocytes was clearly protective (Figure 7E). Thus, each small molecule inhibitor was able to reverse the sensitivity to Fas-induced apoptosis in wild-type and *Timp3*$^{-/-}$ genotypes. The data presented here along with Figures 4 and 5 establish TIMP3 as a regulator of MAPK activity during death receptor activation. Specifically, the loss of *Timp3* shifts the profile of the MAPK cascade, simultaneously inhibiting JNK activation while enhancing ERK1/2 phosphorylation to ultimately promote survival.

Adenoviral ADAM17 prevents acute liver failure in drug-induced toxicity. Hepatotoxicity driven by acetaminophen (APAP) overdose is the most common cause of death by acute liver failure in patients upon hospitalization (44–47). Fas signaling plays a key role in this clinical setting (48–50). We therefore investigated the hepatoprotective potential of ADAM17 in wild-type mice treated with a lethal dose of APAP (600 mg/kg, i.p.). Adenoviruses encoding *Gfp* (*Ad-GFP*) or *Adam17* (*Ad-ADAM17*) were administered at 1×10^9 PFU/ml 96 hours prior to APAP treatment. Successful expression of ADAM17 was assayed via immunoblotting (Figure 8). While a significant proportion of *Ad-GFP*–expressing mice (6 of 9) succumbed to APAP-induced hepatotoxicity, all mice expressing *Ad-ADAM17* (10 of 10) survived APAP treatment (Figure 8A, $P = 0.013$, log-rank test). Measuring hepatotoxicity by serum ALT and histological examination of the 2 groups of mice revealed that *Ad-ADAM17* provided significant protection against APAP overdose (Figure 8, B and C). Extensive necrosis and cellular and structural damage were only observed in the livers of *Ad-GFP*–expressing mice at survival end point (Figure 8C). Next, induction of apoptosis was measured via immunohistochemical staining for active caspase-3 and immunoblotting for caspase-8 and -3. We observed that delivery of adenoviral ADAM17 protected the liver against APAP-induced caspase activation (Figure 8, D and E). Cumulatively, these findings strikingly demonstrate that ADAM17 delivery prevents liver failure in clinically relevant acute hepatitis that relies on Fas signaling.

Discussion

Induction of stress signaling by Fas causes fulminant hepatitis, where the combined cytokine and growth factor availability in the microenvironment contributes to promotion or prevention of cell death. This challenge engages multiple pathways, and cell surface proteolysis presents an attractive interface to integrate them. We show that, individually, TNF, TNFR1, and TIMP3 sensitize the liver to Fas-mediated hepatotoxicity, and that ADAM17 and EGFR protect against this insult. TIMP3 is the sole physiological inhibitor of ADAM17, and the results in *Timp3*$^{-/-}$ mice highlight how ADAM17-mediated ectodomain shedding simultaneously regulates TNF and EGF signaling during a stress response. Enhanced TNFR1 shedding ablates proapoptotic JNK phosphorylation and caspase cleavage in *Timp3*$^{-/-}$ mice. The complete protection observed in compound *Timp3* and *Tnf/Tnfr1* mutant mice treated with Jo-2 further reveals a significant role for ERK1/2-mediated survival signaling in hepatoprotection. We identify what we believe to be a novel function of TIMP3 in negative regulation of EGFR signaling, where *Timp3*$^{-/-}$ cells exhibit elevated release of the EGFR ligands amphiregulin, TGF-α, and HB-EGF, constitutively enhancing EGFR and ERK1/2 phosphorylation. Together, these data constitute the first demonstration to our knowledge that ectodomain shedding serves a powerful function in modulating MAPK cascades during acute hepatic stress.

In vivo hepatotoxicity manifests upon viral infection, chronic inflammation, or fulminant hepatic failure (25, 47). Given the crucial function of the liver in host defense, hepatocytes are highly sensitive to cell-extrinsic cues such as TNF release by activated resident macrophages (Kupffer cells). Recent work by a number of groups has revealed that activators of NF-κB, specifically the IKKγ/NEMO regulatory subunit, can dictate the basal metabolic state of hepatocytes and consequently their capacity to convert extracellular cues into cell-intrinsic signal transduction during chronic and acute inflammation, death receptor activation, and infection (51–53). In addition to the shifted MAPK activation, we observed significantly blunted NF-κB activation and proinflammatory target gene expression in livers of *Timp3*$^{-/-}$ mice that were treated with Jo-2. Consistent with our observations, Beraza et al. (51) report that hepatocyte-specific deletion of *Ikbkg* (IKKγ/NEMO) protects mice from Jo-2–induced fulminant hepatitis, corroborated with a decrease in both stress kinase activation and proinflammatory gene induction. Independent reports demonstrate that deletion of *Ikbkb* (IKKβ), *Ikbkg* (IKKγ/NEMO), or *Rela* (RelA/p65) promotes inflammation-driven hepatocarcinogenesis and sensitizes mice to TNF-induced hepatocyte damage (54, 55). Along with this current study, our previous findings that *Timp3*$^{-/-}$ mice are more sensitive to LPS-induced septic shock and fail to regenerate liver mass upon partial hepatectomy support the hypothesis that when left unchecked, ectodomain shedding deregulates TNF signaling in the liver (22, 23, 36).

As modeled in Figure 9, the current study shows that in addition to impacting TNF signaling, ADAM17 activity in hepatocytes is essential for EGFR ligand release and promotes their paracrine and/or autocrine survival signaling. Engagement of TNFR1 recruits stress kinases and NF-κB, which in turn upregulate proapoptotic mediators such as *Bim* and caspases (refs. 56–58 and Figure 9C). Meanwhile, EGFR activation acts in an opposing manner to promote cell survival by induction of antiapoptotic genes and suppression of *Bim* (refs. 41–43, 59, 60, and Figure 9D). Therefore, the protective mechanism of ADAM17-mediated EGFR activation may be to increase EGFR ligand availability, which in turn induces gene transcription of prosurvival factors. Physiologically, TIMP3 acts to regulate these

opposing pathways by inhibiting the shedding of TNFR1 and EGFR ligands (Figure 9E). The role of ADAM17 in TNF-induced hepatitis was confirmed by in a study by Horiuchi et al. (61), where Mx1-*Cre*–driven loss of *Adam17* in both myeloid cells and hepatocytes or LysM-*Cre*–driven loss in myeloid cells conferred resistance to endotoxin shock by abrogating the delivery of TNF. We propose that when TNF acts as a secondary sensitizer, the availability of TNFRs and parallel activation of other pathways dictate the extent of hepatotoxicity. Significantly, blocking EGFR signaling by the depletion of amphiregulin in fibroblasts and hepatocytes or small molecule inhibition of EGFR and ERK1/2 reversed the protection provided by greater ectodomain shedding. In addition to genetic models, our in vivo experiments conducted with these inhibitors confirmed that countering JNK phosphorylation alleviates hepatotoxicity, while blocking EGFR activation resensitizes *Timp3*$^{-/-}$ mice. Overall, the stress response to increased TNF superfamily ligands may depend on the repertoire of cell surface receptors available to transmit these signals and additional factors in the tissue microenvironment that promote or counteract death receptor activation.

TRAIL is also reported to promote Fas-mediated hepatotoxicity through JNK and Bim in primary hepatocytes and the liver (7). We provide physiological evidence here that TNF itself operates in a similar manner in vivo. Since TNF and TRAIL can activate opposing signal transduction through FADD and NF-κB, the parallel induction of yet other pathways can tip the cellular response to survival or death. The prosurvival role of AKT has been well documented, and its capacity to antagonize JNK may contribute to protection (29, 62). Our probing of AKT activity led us to conclude that *Timp3*$^{-/-}$ cells do not utilize this pathway during hepatotoxicity, since no increase in phosphorylated AKT was observed in TIMP3-deficient tissues subjected to apoptotic stress. Our results provide insight into EGFR activation and ERK1/2 signal transduction in a TIMP3-deficient state, which commits hepatocytes to survival following Fas-mediated toxicity. In support of this interpretation, the protective role of the EGFR pathway is demonstrated in models of stress induced by UV and ROS (10, 63), and a proapoptotic role of TIMP3 in Fas-mediated apoptosis has been suggested in neuronal and synovial fibroblast models in vitro (64, 65). Our finding that dampened TNFR1 activation coupled with enhanced EGFR signaling is protective against acute hepatic failure is consistent with observations that individually, ablating JNK signaling or elevating EGFR activation can protect, at least in part, against receptor-mediated apoptosis (7, 9). While proapoptotic and prosurvival kinases can operate in isolation, it is unlikely that this is the case during physiological stress. The reported intracellular crosstalk between JNK and ERK1/2 is another level at which the apoptotic response can be shifted (66, 67). While our observations are within the context of death receptor activation during acute stress, the coordination of opposing signal transduction pathways applies to numerous aspects of hepatic homeostasis. A recent review by Michalopoulos discusses the other coordinating signals during liver regeneration and importantly liver failure upon loss of this regulation (68).

Fulminant hepatitis is a significant cause of drug-induced liver failure and also contributes to the hepatotoxicity observed in steatosis and end-stage liver disease. Our findings show that ectodomain shedding promotes hepatocyte survival in this acute setting by the dual mechanism of enhanced EGFR-ERK1/2 activation and dampened TNFR1 signaling through JNK and NF-κB. We further demonstrate that adenoviral delivery of ADAM17 is capable of protecting mice from APAP-induced liver failure. Even though unchecked metalloproteinase activity is implicated in chronic hepatic inflammation, inducing transient ectodomain shedding may be an attractive strategy to limit toxicity during fulminant liver failure.

Methods

Mice. All mice used in this study were of the C57BL/6 background. Male mice aged 9–12 weeks were used for all the experimental procedures. *Timp3*$^{-/-}$ mice have been previously described (22), and *Tnf*$^{-/-}$ and *Tnfr1*$^{-/-}$ mice were obtained from The Jackson Laboratory. These strains were crossed with *Timp3*$^{-/-}$ mice to generate *Timp3*$^{-/-}$*Tnf*$^{-/-}$ and *Timp3*$^{-/-}$*Tnfr1*$^{-/-}$ mice. Hepatocyte-specific knockouts were produced by crossing mice expressing *Cre* recombinase under the albumin promoter (The Jackson Laboratory) with *Adam17*$^{fl/fl}$ or *Egfr*$^{fl/fl}$ mice. Genotypes were confirmed via PCR for the respective genes; primer sequences are provided in Supplemental Table 1. Mice were fed 5%-fat chow ad libitum and housed and cared for in accordance with protocols approved by the Canadian Council for Animal Care and the Animal Care Committee of the Ontario Cancer Institute.

Fas-induced hepatotoxicity. Mice were injected i.p. with Fas-agonist antibody (CD95, clone Jo-2, NA/LE) in 100 μl sterile PBS to trigger death receptor activation. Since Jo-2 exhibits lot-to-lot variation in its potency of hepatocyte killing, we tested 3 lots and identified BD Biosciences — Pharmingen 554254 at 0.65 μg/g mouse weight to cause morbidity within 5–7 hours in wild-type mice. Control mice were injected with 100 μl sterile PBS. For JNK inhibition experiments, wild-type mice were injected i.p. with 0.25 μg/g SP600125 (Calbiochem) 45 minutes prior to Jo-2 injection. For EGFR inhibition experiments, *Timp3*$^{-/-}$ mice were injected i.p. with 0.50 μg/g erlotinib 1 hour prior to Jo-2 injection (erlotinib provided by Ming-Sound Tsao, Ontario Cancer Institute). PBS containing 10% DMSO was used as a vehicle. Animals were sacrificed by CO_2 asphyxiation at designated time points for analysis. Survival curves were obtained based on the time at which animals became premoribund. Hepatotoxicity was determined by measuring serum ALT levels.

APAP-induced hepatotoxicity and adenoviral delivery of ADAM17. To obtain an optimal proportion of adenovirus-infected hepatocytes, a dose titration of Ad-GFP (Vector Biolabs) was performed in wild-type mice at 1×10^7, 1×10^8, and 1×10^9 PFU/ml dissolved in 500 μl sterile PBS. Administration of 1×10^9 PFU/ml of Ad-GFP showed a significantly higher proportion of GFP-positive hepatocytes compared with 1×10^7 or 1×10^8 PFU/ml titers. Thus, 1×10^9 PFU/ml Ad-GFP and Ad-ADAM17 were dissolved in sterile PBS and delivered intravenously in the tail veins of 12-week-old male mice. Ninety-six hours after injection of virus, mice were starved for 18 hours prior to APAP injections (Sigma-Aldrich, A5000). APAP was dissolved in sterile PBS and warmed to 55°C to dissolve, and 600 mg/kg dosed in 200 μl PBS was i.p. injected into mice. Survival curves were obtained based on the pre-moribund status of animals, at which point they were sacrificed. Liver, kidney, and serum were obtained for subsequent analyses.

Primary hepatocyte culture and apoptosis assays. Primary hepatocytes were prepared by perfusing the portal vein of the liver with 0.02 mg/ml Liberase (Roche) and enriched using a 10% Percoll (Sigma-Aldrich) gradient. Hepatocytes were cultured in William's E medium containing 10% fetal bovine serum, 2 mM L-glutamine, 0.1 U/ml insulin, 1.0 mM dexamethasone, and antibiotics on 6-well plates coated with 2.5 mg/ml type I rat tail collagen. Hepatocytes (1×10^6/well, 6-well plate) were serum starved for 24 hours, then treated with 10 ng/ml Fas agonist antibody (Jo-2, BD Biosciences) in the presence or absence of 1 ng/ml recombinant mouse TNF (R&D Systems) for the indicated time points. Media and cell lysate were collected for analysis. Hepatocytes were coincubated with small molecule inhibitors of ADAM17 (10 μM TAPI-1, Peptides International), JNK (25 μM SP600125, Calbiochem), EGFR (100 nM erlotinib), and MEKK (10 μM U0126, Sigma-Aldrich) where indicated. For conditioned media (CM) experiments, culture media was obtained from MEFs of indicated genotypes that were stimu-

lated with 1.0 μM LPA for 1 hour. Wild-type hepatocytes were incubated with CM 3 hours prior to addition of 1 ng/ml TNF plus 10 ng/ml Jo-2. CM was maintained in a 1:1 dilution with hepatocyte media containing TNF plus Jo-2 during induction of apoptosis for another 3 hours, after which cell lysate was collected for analysis. *Timp3*$^{-/-}$ hepatocytes were incubated with 5.0 μg/ml IgG or αAR (AF989, R&D Systems) 3 hours prior to addition of 1 ng/ml TNF plus 10 ng/ml Jo-2. Antibodies were maintained in hepatocyte culture media during induction of apoptosis for another 3 hours. Cell lysate was collected for analysis of caspase-3/7 activity.

LPA treatment of MEFs. Primary MEFs were generated as described previously (69) and cultured in DMEM with 10% fetal bovine serum and antibiotics. MEFs were cultured until 80% confluent and starved for 48 hours prior to treatment. Cells were incubated for 30 minutes with 0.03 μM, 0.1 μM, or 1.0 μM LPA (Sigma-Aldrich, L7260) dissolved in sterile water. MEFs were incubated with 50 ng/ml recombinant human EGF (BD Biosciences) for 15 minutes as positive controls of EGFR phosphorylation and ERK1/2 phosphorylation. Where indicated, MEFs were preincubated with 10 μM TAPI-1 (Peptides International) or 1 μM erlotinib dissolved in DMSO for 1 hour, then incubated with the indicated concentrations of LPA for 15 minutes in the presence of inhibitor. Two independent fibroblast lines from wild-type embryos and 4 lines from *Timp3*$^{-/-}$ embryos were stimulated with LPA as described to measure EGFR signaling. For amphiregulin neutralization experiments, *Timp3*$^{-/-}$ MEFs were pretreated with 50.0 μg/ml IgG or αAR(R&D Systems) for 2 hours. Cells were then treated with 1.0 μM LPA for an additional 5 minutes. Media and cell lysate were collected for analysis.

Immunoblotting. Total liver protein was extracted by mortar and pestle homogenization of frozen tissue. RIPA extraction buffer containing 25 mM Tris-HCl pH 7.6, 1% Triton X-100, 0.1% SDS, 1% NP-40, 1% sodium deoxycholate, 5 mM EDTA, 50 mM NaCl, 200 μM Na_3VO_4, 2 mM PMSF, and an appropriate dilution of Complete Mini, EDTA-free protease inhibitor cocktail tablets (Roche) was used to lyse all tissue and cells, and lysate was stored at –70°C. Protein (15–50 μg) was loaded on SDS-PAGE gels for Western blotting. The following anti-mouse antibodies were used: anti–phosphorylated JNK (p-JNK, Thr183/Tyr185), anti-JNK, anti–phosphorylated p44/42 MAPK (p-ERK1/2, Thr202/Tyr204), anti–p44/42 MAPK (ERK1/2), anti–p38 MAPK, anti–phosphorylated p38 MAPK (p-p38, Thr180/Tyr182), anti-EGFR, anti–phosphorylated EGFR (p-EGFR, Tyr1173), anti-AMPKβ, anti–phosphorylated AMPKβ (p-AMPKβ, Ser108), anti-AKT, anti–phosphorylated AKT (p-AKT, Ser473), anti–caspase-3, anti–caspase-9 (all from Cell Signaling Technology), anti–caspase-8 (R&D Systems), TACE/ADAM17 specific for the disintegrin domain (produced in-house), and anti–β-actin (Santa Cruz Biotechnology Inc.).

Caspase activity assays. Fluorometric caspase activity assays were performed using 15 μg protein and 20 μM fluorescent substrates (caspase-3/7: Ac-DEVD-AMC, caspase-9: Ac-LEHD-AMC; AnaSpec Inc.). Protein and substrates were incubated for 60 minutes and fluorescence emission measured at 352 nm every 5 minutes for 1 hour to obtain kinetic measurement of enzymatic activity.

EMSA. NF-κB activity in liver tissue was determined by EMSA using a common NF-κB biotinylated nucleic acid probe (Panomics) on nuclear fractions of livers. Briefly, liver tissue was homogenized in buffer A (10 mM HEPES pH 7.9, 1.5 mM $MgCl_2$, 10 mM KCl, protease inhibitors) and centrifuged to isolate nuclear pellet. The pellet was resuspended in buffer B (20 mM HEPES pH 7.9, 1.5 mM $MgCl_2$, 420 mM NaCl, 0.2 mM EDTA, 25% v/v glycerol, protease inhibitors). After centrifugation, the supernatant containing nuclear extract was collected and stored at –70°C. EMSA was performed according to the supplier's protocol (Panomics).

ELISA. For serum ELISA, blood was collected from mice by cardiac puncture upon sacrifice at the indicated time points. Serum was isolated from whole blood by centrifugation (BD Vacutainer CPT Cell Preparation Tube). Serum was diluted 1:200 for TNFR1 and TNFR2 ELISA and 1:10 for Fas, Fas ligand, and TNF. Undiluted media was used for assays on cell culture experiments. ELISA was performed as per the manufacturers' instructions (TNFR1, Fas, Fas ligand, amphiregulin, HB-EGF, TGF-α from R&D Systems; TNFR2, TNF from BD Biosciences — Pharmingen).

Histology and immunohistochemistry. Liver lobes were fixed in 5% formalin for 24 hours, transferred to PBS, and processed for embedding in paraffin. Five-micrometer sections were placed on Superfrost/Plus microscope slides (Fisher Scientific) and processed as previously described (22). The following stains were applied for immunohistochemical analysis: Harris' hematoxylin (Electron Microscopy Sciences) and eosin (Fisher Scientific). Anti–cleaved caspase-3 antibody (Cell Signaling Technology) was used according to the manufacturer's specifications.

RNA preparation and quantitative RT-PCR. RNA was prepared from frozen liver tissue using TRIzol reagent (Invitrogen) according to the manufacturer's instructions. cDNA was obtained using a first-strand cDNA synthesis protocol (Promega). Gene expression was measured using SYBR Green reagent (Quanta) or Taqman primer/probesets (Applied Biosystems) in a 7800HT real-time PCR system (Applied Biosciences). All gene expression levels were normalized to *Actb* (β-*actin*, SYBR Green) or *Rn18s* (*18S*, Taqman), and fold change was measured relative to control wild-type samples. qRT-PCR of RNA was used as a negative control. The amount of each product was calculated using the $2^{-\Delta\Delta CT}$ method. Primer sequences and Taqman primer/probeset IDs are provided in Supplemental Table 1.

Statistics. Data are reported as mean ± SD or SEM. All calculations were carried out using GraphPad Prism software (GraphPad Software). Comparisons were made by 2-tailed Student's *t* test and ANOVA; comparisons between Kaplan-Meier survival curves were made by log-rank test.

Acknowledgments

The authors thank Swami Naralareddy for technical assistance, Geoffrey A. Wood for histopathology analysis, and Razquallah Hakem and Paul Waterhouse for constructive criticism of the manuscript. A. Murthy is supported by a Frederick Banting and Charles Best Canada Graduate Scholarship from the Canadian Institutes of Health Research, and this work is supported by funding to the R. Khokha laboratory from the Canadian Institutes of Health Research.

Received for publication February 16, 2010, and accepted in revised form May 19, 2010.

Address correspondence to: Rama Khokha, Ontario Cancer Institute, 610 University Avenue, Toronto, Ontario M5G 2M9, Canada. Phone: 416.946.2051; Fax: 416.946.2984; E-mail: rkhokha@uhnres.utoronto.ca.

1. Kaufmann T, et al. Fatal hepatitis mediated by tumor necrosis factor TNFalpha requires caspase-8 and involves the BH3-only proteins Bid and Bim. *Immunity*. 2009;30(1):56–66.
2. Das M, Sabio G, Jiang F, Rincon M, Flavell RA, Davis RJ. Induction of hepatitis by JNK-mediated expression of TNF-alpha. *Cell*. 2009;136(2):249–260.
3. Grivennikov SI, et al. Distinct and nonredundant in vivo functions of TNF produced by t cells and macrophages/neutrophils: protective and deleterious effects. *Immunity*. 2005;22(1):93–104.
4. Aggarwal BB. Signalling pathways of the TNF superfamily: a double-edged sword. *Nat Rev Immunol*. 2003;3(9):745–756.
5. Chen X, et al. Bid-independent mitochondrial activation in tumor necrosis factor alpha-induced apoptosis and liver injury. *Mol Cell Biol*. 2007;27(2):541–553.
6. Hughes PD, Belz GT, Fortner KA, Budd RC, Strasser A, Bouillet P. Apoptosis regulators Fas and Bim cooperate in shutdown of chronic immune responses and prevention of autoimmunity. *Immunity*. 2008;28(2):197–205.
7. Corazza N, et al. TRAIL receptor-mediated JNK

activation and Bim phosphorylation critically regulate Fas-mediated liver damage and lethality. *J Clin Invest*. 2006;116(9):2493–2499.
8. Miettinen PJ, et al. Epithelial immaturity and multiorgan failure in mice lacking epidermal growth factor receptor. *Nature*. 1995;376(6538):337–341.
9. Berasain C, et al. Novel role for amphiregulin in protection from liver injury. *J Biol Chem*. 2005;280(19):19012–19020.
10. Fischer OM, Hart S, Gschwind A, Prenzel N, Ullrich A. Oxidative and osmotic stress signaling in tumor cells is mediated by ADAM proteases and heparin-binding epidermal growth factor. *Mol Cell Biol*. 2004;24(12):5172–5183.
11. Eberle A, Reinehr R, Becker S, Haussinger D. Fluorescence resonance energy transfer analysis of proapoptotic CD95-EGF receptor interactions in Huh7 cells. *Hepatology*. 2005;41(2):315–326.
12. Khai NC, et al. In vivo hepatic HB-EGF gene transduction inhibits Fas-induced liver injury and induces liver regeneration in mice: a comparative study to HGF. *J Hepatol*. 2006;44(6):1046–1054.
13. Musallam L, Ethier C, Haddad PS, Bilodeau M. EGF mediates protection against Fas-induced apoptosis by depleting and oxidizing intracellular GSH stocks. *J Cell Physiol*. 2004;198(1):62–72.
14. Reinehr R, Schliess F, Haussinger D. Hyperosmolarity and CD95L trigger CD95/EGF receptor association and tyrosine phosphorylation of CD95 as prerequisites for CD95 membrane trafficking and DISC formation. *FASEB J*. 2003;17(6):731–733.
15. Black RA, et al. A metalloproteinase disintegrin that releases tumour-necrosis factor-alpha from cells. *Nature*. 1997;385(6618):729–733.
16. Peschon JJ, et al. An essential role for ectodomain shedding in mammalian development. *Science*. 1998;282(5392):1281–1284.
17. Blobel CP. ADAMs: key components in EGFR signalling and development. *Nat Rev Mol Cell Biol*. 2005;6(1):32–43.
18. Sahin U, et al. Distinct roles for ADAM10 and ADAM17 in ectodomain shedding of six EGFR ligands. *J Cell Biol*. 2004;164(5):769–779.
19. Lee DC, et al. TACE/ADAM17 processing of EGFR ligands indicates a role as a physiological convertase. *Ann N Y Acad Sci*. 2003;995:22–38.
20. Nagase H, Visse R, Murphy G. Structure and function of matrix metalloproteinases and TIMPs. *Cardiovasc Res*. 2006;69(3):562–573.
21. Wisniewska M, et al. Structural determinants of the ADAM inhibition by TIMP-3: crystal structure of the TACE-N-TIMP-3 complex. *J Mol Biol*. 2008;381(5):1307–1319.
22. Mohammed FF, et al. Abnormal TNF activity in Timp3–/– mice leads to chronic hepatic inflammation and failure of liver regeneration. *Nat Genet*. 2004;36(9):969–977.
23. Smookler DS, Mohammed FF, Kassiri Z, Duncan GS, Mak TW, Khokha R. Tissue inhibitor of metalloproteinase 3 regulates TNF-dependent systemic inflammation. *J Immunol*. 2006;176(2):721–725.
24. Tsuji H, et al. Tumor necrosis factor receptor p55 is essential for intrahepatic granuloma formation and hepatocellular apoptosis in a murine model of bacterium-induced fulminant hepatitis. *Infect Immun*. 1997;65(5):1892–1898.
25. O'Grady JG, Schalm SW, Williams R. Acute liver failure: redefining the syndromes. *Lancet*. 1993; 342(8866):273–275.
26. Menghini R, et al. Tissue inhibitor of metalloproteinase 3 deficiency causes hepatic steatosis and adipose tissue inflammation in mice. *Gastroenterology*. 2009;136(2):663–672.
27. Chang L, et al. The E3 ubiquitin ligase itch couples JNK activation to TNFalpha-induced cell death by inducing c-FLIP(L) turnover. *Cell*. 2006;124(3):601–613.
28. Kamata H, Honda S, Maeda S, Chang L, Hirata H, Karin M. Reactive oxygen species promote TNFalpha-induced death and sustained JNK activation by inhibiting MAP kinase phosphatases. *Cell*. 2005;120(5):649–661.
29. Morel C, Carlson SM, White FM, Davis RJ. Mcl-1 integrates the opposing actions of signaling pathways that mediate survival and apoptosis. *Mol Cell Biol*. 2009;29(14):3845–3852.
30. Javelaud D, Besancon F. NF-kappa B activation results in rapid inactivation of JNK in TNF alpha-treated Ewing sarcoma cells: a mechanism for the anti-apoptotic effect of NF-kappa B. *Oncogene*. 2001;20(32):4365–4372.
31. Liu J, Lin A. Role of JNK activation in apoptosis: a double-edged sword. *Cell Res*. 2005;15(1):36–42.
32. Wicovsky A, et al. Sustained JNK activation in response to tumor necrosis factor is mediated by caspases in a cell type-specific manner. *J Biol Chem*. 2007;282(4):2174–2183.
33. Luo JL, Maeda S, Hsu LC, Yagita H, Karin M. Inhibition of NF-kappaB in cancer cells converts inflammation- induced tumor growth mediated by TNFalpha to TRAIL-mediated tumor regression. *Cancer Cell*. 2004;6(3):297–305.
34. Vallabhapurapu S, Karin M. Regulation and function of NF-kappaB transcription factors in the immune system. *Annu Rev Immunol*. 2009;27:693–733.
35. Maurer U, Charvet C, Wagman AS, Dejardin E, Green DR. Glycogen synthase kinase-3 regulates mitochondrial outer membrane permeabilization and apoptosis by destabilization of MCL-1. *Mol Cell*. 2006;21(6):749–760.
36. Black RA. TIMP3 checks inflammation. *Nat Genet*. 2004;36(9):934–935.
37. Lee MH, Knauper V, Becherer JD, Murphy G. Full-length and N-TIMP-3 display equal inhibitory activities toward TNF-alpha convertase. *Biochem Biophys Res Commun*. 2001;280(3):945–950.
38. Natarajan A, Wagner B, Sibilia M. The EGF receptor is required for efficient liver regeneration. *Proc Natl Acad Sci U S A*. 2007;104(43):17081–17086.
39. Daub H, Wallasch C, Lankenau A, Herrlich A, Ullrich A. Signal characteristics of G protein-transactivated EGF receptor. *EMBO J*. 1997;16(23):7032–7044.
40. Gschwind A, Hart S, Fischer OM, Ullrich A. TACE cleavage of proamphiregulin regulates GPCR-induced proliferation and motility of cancer cells. *EMBO J*. 2003;22(10):2411–2421.
41. Alfano D, Iaccarino I, Stoppelli MP. Urokinase signaling through its receptor protects against anoikis by increasing BCL-xL expression levels. *J Biol Chem*. 2006;281(26):17758–17767.
42. Faber AC, et al. Differential induction of apoptosis in HER2 and EGFR addicted cancers following PI3K inhibition. *Proc Natl Acad Sci U S A*. 2009; 106(46):19503–19508.
43. Leu CM, Chang C, Hu C. Epidermal growth factor (EGF) suppresses staurosporine-induced apoptosis by inducing mcl-1 via the mitogen-activated protein kinase pathway. *Oncogene*. 2000;19(13):1665–1675.
44. Henderson NC, et al. Critical role of c-jun (NH2) terminal kinase in paracetamol- induced acute liver failure. *Gut*. 2007;56(7):982–990.
45. Imaeda AB, et al. Acetaminophen-induced hepatotoxicity in mice is dependent on Tlr9 and the Nalp3 inflammasome. *J Clin Invest*. 2009;119(2):305–314.
46. Lee WM. Acetaminophen toxicity: changing perceptions on a social/medical issue. *Hepatology*. 2007;46(4):966–970.
47. Malhi H, Gores GJ, Lemasters JJ. Apoptosis and necrosis in the liver: a tale of two deaths? *Hepatology*. 2006;43(2 suppl 1):S31–44.
48. Tagami A, Ohnishi H, Hughes RD. Increased serum soluble Fas in patients with acute liver failure due to paracetamol overdose. *Hepatogastroenterology*. 2003;50(51):742–745.
49. Tinel M, et al. Subliminal Fas stimulation increases the hepatotoxicity of acetaminophen and bromobenzene in mice. *Hepatology*. 2004;39(3):655–666.
50. Zhang H, et al. Reduction of liver Fas expression by an antisense oligonucleotide protects mice from fulminant hepatitis. *Nat Biotechnol*. 2000;18(8):862–867.
51. Beraza N, et al. Hepatocyte-specific NEMO deletion promotes NK/NKT cell- and TRAIL-dependent liver damage. *J Exp Med*. 2009;206(8):1727–1737.
52. Luedde T, et al. Deletion of NEMO/IKKgamma in liver parenchymal cells causes steatohepatitis and hepatocellular carcinoma. *Cancer Cell*. 2007;11(2):119–132.
53. Sun B, Karin M. NF-kappaB signaling, liver disease and hepatoprotective agents. *Oncogene*. 2008; 27(48):6228–6244.
54. Geisler F, Algul H, Paxian S, Schmid RM. Genetic inactivation of RelA/p65 sensitizes adult mouse hepatocytes to TNF-induced apoptosis in vivo and in vitro. *Gastroenterology*. 2007;132(7):2489–2503.
55. Maeda S, Kamata H, Luo JL, Leffert H, Karin M. IKKbeta couples hepatocyte death to cytokine-driven compensatory proliferation that promotes chemical hepatocarcinogenesis. *Cell*. 2005;121(7):977–990.
56. Inta I, et al. Bim and Noxa are candidates to mediate the deleterious effect of the NF-kappa B subunit RelA in cerebral ischemia. *J Neurosci*. 2006;26(50):12896–12903.
57. Ghosh S, May MJ, Kopp EB. NF-kappa B and Rel proteins: evolutionarily conserved mediators of immune responses. *Annu Rev Immunol*. 1998;16:225–260.
58. Song L, et al. IKKbeta programs to turn on the GADD45alpha-MKK4-JNK apoptotic cascade specifically via p50 NF-kappaB in arsenite response. *J Cell Biol*. 2006;175(4):607–617.
59. Gong Y, et al. Induction of BIM is essential for apoptosis triggered by EGFR kinase inhibitors in mutant EGFR-dependent lung adenocarcinomas. *PLoS Med*. 2007;4(10):e294–e294.
60. Reginato MJ, et al. Integrins and EGFR coordinately regulate the pro-apoptotic protein Bim to prevent anoikis. *Nat Cell Biol*. 2003;5(8):733–740.
61. Horiuchi K, et al. Cutting edge: TNF-alpha-converting enzyme (TACE/ADAM17) inactivation in mouse myeloid cells prevents lethality from endotoxin shock. *J Immunol*. 2007;179(5):2686–2689.
62. Kim AH, Khursigara G, Sun X, Franke TF, Chao MV. Akt phosphorylates and negatively regulates apoptosis signal-regulating kinase 1. *Mol Cell Biol*. 2001;21(3):893–901.
63. Berasain C, et al. Amphiregulin: an early trigger of liver regeneration in mice. *Gastroenterology*. 2005;128(2):424–432.
64. Drynda A, et al. Gene transfer of tissue inhibitor of metalloproteinases-3 reverses the inhibitory effects of TNF-alpha on Fas-induced apoptosis in rheumatoid arthritis synovial fibroblasts. *J Immunol*. 2005;174(10):6524–6531.
65. Wetzel M, et al. Tissue inhibitor of metalloproteinases-3 facilitates Fas-mediated neuronal cell death following mild ischemia. *Cell Death Differ*. 2008;15(1):143–151.
66. Junttila MR, Li SP, Westermarck J. Phosphatase-mediated crosstalk between MAPK signaling pathways in the regulation of cell survival. *FASEB J*. 2008;22(4):954–965.
67. Xia Z, Dickens M, Raingeaud J, Davis RJ, Greenberg ME. Opposing effects of ERK and JNK-p38 MAP kinases on apoptosis. *Science*. 1995;270(5240):1326–1331.
68. Michalopoulos GK. Liver regeneration after partial hepatectomy: critical analysis of mechanistic dilemmas. *Am J Pathol*. 2010;176(1):2–13.
69. English JL, et al. Individual Timp deficiencies differentially impact pro-MMP-2 activation. *J Biol Chem*. 2006;281(15):10337–10346.